FUNCTIONAL CHARACTERIZATION OF PUTATIVE MITOTIC BOOKMARKING FACTORS IN PLURIPOTENCY MAINTENANCE

FUNCTIONAL CHARACTERIZATION OF PUTATIVE MITOTIC BOOKMARKING FACTORS IN PLURIPOTENCY MAINTENANCE

By

XIAOXIAO (DAISY) DENG, B. Sc. Hons

A Thesis Submitted to the School of Graduate Studies in Partial Fulfillment of the Requirements for the Degree Master of Science

McMaster University

Descriptive Note

McMaster University Master of Science (2018) Hamilton, Ontario

TITLE: Functional Characterization of Putative Mitotic Bookmarking Factors in Pluripotency Maintenance

AUTHOR: Xiaoxiao (Daisy) Deng, B. Sc. Hons (McMaster University)

SUPERVISOR: Dr. Jonathan S. Draper

NUMBER OF PAGES: xi, 67

Abstract

Pluripotent stem cells are a special population of stem cell with indefinitely self-renewal and unlimited differentiation capability, which makes them an attractive avenue for regenerative medicine and disease modeling. Therefore, it is important to understanding the fundamental mechanisms that govern and maintain their pluripotent state. A phenomenon termed mitotic bookmarking has recently been suggested as a potential mechanism involved in the stable propagation of cellular identity through the cell cycles. Candidate-based studies have identified mitotic bookmarking factors that are retained on the mitotic chromatin and preserve the transcriptional memory of the cell. Nevertheless, there is a poor understanding of which proteins can serve as mitotic bookmarks, as well as the chromatin dynamics of bookmarked sites during mitosis and the start of the G1 phase. We have previously identified a list of putative mitotic bookmarking factors in pluripotent stem cells, from which we tested the role of PARP1, HDGF, and PSIP1 as potential bookmarks for the propagation of the pluripotent state through mitosis. Here we showed that the absence of PARP1 at the M-G1 transition impairs self-renewal capability of pluripotent stem cells without affecting the proliferation and cell cycle progression. Conclusive evidence that establishes a role for HDGF or PSIP1 in mitotic bookmarking of pluripotent stem cells has yet to emerge. However, our work provides a new avenue for exploring the functional importance of mitotic bookmarks in pluripotent maintenance.

Acknowledgment

Over the intensive period of two years, today is the day for me to express my gratitude towards everyone who has supported and assisted me in completing one of the signifying milestones in my academic life. It has been a period of intense learning for me, not only in the scientific arena but also on a personal level. Completing my Master's study and compiling this report has had a great impact on me, and I would like to reflect on the people who have provided warm support and substantial assistance that has enabled my academic and personal development throughout this period.

Foremost, I would like to express my sincere gratitude to my Master's supervisor Dr. Jonathan Draper for the endless support he has offered me during my graduate study, for his patient, inspiration, enthusiasm, and immense knowledge. He has provided me with such a great opportunity to join a lab packed with great friendship, learning opportunity, and personal growth. The amount that I have learned in the past two years was beyond what I had expected when I first started. I could not have imagined having a better supervisor and lab environment for my graduate study.

I would also like to thank my committee members, Dr. Karun Singh and Dr. Kristin Hope, who has been extremely supportive and encouraging throughout my study. Beside the supports, I have received enormous insightful and inspirational advice that have significantly supplemented my research project. In addition, I would like to express my special thanks to Dr. Kristin Hope, who has taken up the supervising role during Jon's absence.

In addition, I really appreciated the help and support I have received from my lab colleagues, especially Sonam and Amanda, who have taught me many valuable skills, both technically and transferable. I would also like to acknowledge the contribution many people toward my thesis project, especially Sonam, Amanda, and Ish.

My study would not have been possible without my lovely family, particularly my mom, who has offered me great emotional support during my graduate studies. Mom, you are the most amazing parent one could ask for, and my graduate studies would be much more difficult without your encouragement. Thank you for always being here when I needed you.

Lastly, I would like to thank the staffs at SCCRI and McMaster Biochemistry department, who have provided professional support regarding administrative task during my study, allowing me to focus my attention on actual experiments and course works.

Table of Contents

List of Figures and Tables

Figures

Tables

List of Abbreviations and Symbols

7AAD	7 aminoactinomycin D
AP	Alkaline phosphatase
ATAC-seq	Assay for transposase-accessibility chromatin followed by sequencing
BME	Betamercaptoethanol
BSA	Bovine Serum Albumin
Cas9	CRISPR associated protein 9
Cdks	Cyclin-dependent kinases
ChIP	Chromatin Immunoprecipitation
ChIP-MS	Chromatin immunoprecipitation followed by mass spectrometry
ChIP-seq	Chromatin immunoprecipitation with sequencing
CRISPR	Clustered regularly interspaced short palindromic repeats
CIC	Colony initiation cell
DNase-seq	DNase I sensitivity assay coupled to high-throughput sequencing
DT	Doubling time
EDTA	Ethylenediaminetetraacetic acid
ERK	Extracellular signal-regulated kinase
FACS	Fluorescent activated cell sorting
FGF	Fibroblast growth factor
FLIP	Fluorescence loss in photobleaching
G1	Gap 1
G2	Gap 2
G1t20	G1 populations collected after 20 minutes of release into G1 from mitosis
G1t35	G1 populations collected after 35 minutes of release into G1 from mitosis
G2M	G2 and Mitotic mixed populations
GO	Gene Ontology
H2B	Histone2B
H3	Histone 3
H3K27Ac	Acetylation of histone H3 at lysine 27
H3K36me3	Trimethylation of histone H3 at lysine 36
H3K79me3	Trimethylation of histone H3 at lysine 79
H3S10P	Phosphorylated serine 10 on histone 3
H4K20me3	Trimethylation of histone H4 at lysine 20
hESCs	Human embryonic stem cells
HDGF	Hepatoma-derived growth factor
IgG	Immunoglobulin
IP	Immunoprecipitation
KO	Knockout
LIF	Leukemia inhibitor factor

M	Mitosis
MD	Mitotic degradation domain or mitotic degron
MD^{R24A}	Inactive MD, Arginine at amino acid 42 is substituted with Alanine
mESCs	Mouse embryonic stem cells
mKO2	monomeric Kusabira orange 2
MLL	Mixed Lineage Leukemia
NLS	Nuclear localization signal
RA	Retinoic acid
pADPr	Poly(ADP-ribose)
PARP1	Poly(ADP ribose) polymerase I
PFA	Paraformaldehyde
pRb-E2F	Retinoblastoma protein and E2F transcription factor
PSCs	Pluripotent stem cells
PSIP1	PC4 and SFRS1 interacting protein
PWWP	Proline-Tryptophan-Tryptophan-Proline
RIPA	Radioimmunoprecipitation assay buffer
RNA-seq	RNA-sequencing
RT	Room temperature
RT-qPCR	Quantitative reverse transcription polymerase chain reaction
S	Synthesis
SD	Standard deviation
TADs	Topologically associated domains
WT	Wild-type
xMEFs	x-ray irradiated mouse embryonic fibroblasts

Preface

My thesis focuses on the role mitotic bookmarks plays in cell fate regulation and maintenance in pluripotent stem cells. It can be divided into two parts based on the factors studied.

The first part examines the mitotic bookmarking role of PARP1 in pluripotent maintenance through mitosis. PARP1 was identified in our mitotic bookmarking screen data, and the literature describes PARP1 acting as a bookmarking factor in HEK 293 lines. Our study focuses on how PARP1 bookmarking activity during mitosis is related to the pluripotent state of pluripotent stem cells. Several people have contributed toward various portions of the study. The design and plan of the project were carried out by Dr. Sonam Bhatia, Dr. Jon Draper and myself. I generated PARP1 knockout lines, performed the characterization assays, assisted in the collection of material for mitotic release experiments, and performed majority of the data analysis. The RT-qPCR for accessing transcriptional reactivation of PARP1 knockouts was completed by Sonam, and she has assisted in setting CIC assay for the PARP1 rescue lines, contributing to Figure 7 and 10. Mohammad (Ish) Alam (Dr. Draper's lab) assisted with the fluorescence loss in photobleaching experiments, contributing to Figure 9.

In the second part, we have studied another group of putative mitotic bookmarks, the PWWP-containing factors, HDGF and PSIP. The basis of selecting this group of factors is due to the well-characterized DNA and histone binding activity of the PWWP domain. Although both HDGF and PSIP1 are well studied in term of their role in different tissues, they have yet to be examined in relation to their mitotic bookmarking activity or their role

in pluripotency. I have designed and planned this part along with input from Dr. Jon Draper, and carried out the majority of the experiments. Amanda Hrenczuk generated the HDGF and PSIP1 knockout mESC lines. Mohammad Alam assisted in setting up the CIC assay for HDGF rescue lines and cross-linked chromatin immunoprecipitation, contribution to Figure 12 and 13.

1.1 Introduction

1.1.1 Introduction to pluripotency and cell cycle

Pluripotent stem cells (PSCs) are derived from the inner cell mass of a blastocyst-stage embryo and can be defined by their unique ability to indefinitely self-renewal while retaining the potential to differentiate into all three germ lineages: endoderm, mesoderm, and ectoderm[1, 2]. The self-renewal and differentiation capability of PSCs make them a powerful tool for various applications, including drug discovery and disease modeling. Since the discovery of PSCs, researchers have invested in decoding the molecular basis of pluripotency, as it is fundamental to the understanding of stem cell biology, embryonic development, and possible clinical application of regenerative medicine. Studies have gradually revealed that a complex network of factors, including transcription factors and epigenetic regulators, is responsible for regulating pluripotency through multiple signaling transduction pathways. The generally accepted core pluripotency factors include OCT4[3], NANOG[4], and SOX2[5], as reintroducing these factors can induce a pluripotent state in somatic cells[6]. Current evidence suggests that reprogramming of somatic cells requires cell division[7], and a high proliferation rate[8] is directly linked to increasing reprogramming efficiency, suggesting the important role cell cycle regulation plays in the establishing the pluripotent identity.

The eukaryotic cell cycle is consist of four tightly regulated distinct phases (G1, S, G2, M) dedicated to the replication and transmission of genetic material from the parental cell to its progeny[9]. The synthesis (S) phase and mitosis (M) are periods where DNA

replication and transmission occurs, respectively. The two gap phases (G1 and G2) temporally separate S from M phase, allowing the cell to make decision and preparation to undergo cell division. The G1, S, and G2 phase comprise the transcriptional active interphase, and M phase is where the cell division occurs. Cell division and cell cycle progression are precisely controlled by mechanisms that ensure the chromosomal DNA are faithfully replicated, and then distributed equally to each daughter cell. Two classes of molecules[9-13], cyclin-dependent kinases (Cdks), a family of serine/threonine kinases, and their binding partners, cyclins, play a key role to ensure that the four cell cycle phases are maintained in the correct temporal order. The cell cycle progression can be characterized by overlapping waves of phase-specific Cdk activities[10], which then activate or inactivate target proteins to promote cell cycle progression. For instance, the M phase Cdk1-cycle B[11] complexes drive mitosis but inhibit cytokinesis and DNA replication. The activation of Cdk activity requires the assembly of Cdk with its regulatory cyclin partner[12-13]. Cyclins are unstable proteins that are synthesized and degraded at precise times during the cell cycle, thus generating waves of Cdk activity[14]. Therefore, the precise timing of cyclin accumulation is critical for normal cell cycle progression, and dysregulation can adversely affect genomic integrity and growth control.

In contrast to most somatic cells, PSCs, including mouse embryonic stem cells (mESCs) and human embryonic stems cells (hESCs)[15-17], exhibit unusually cell cycle features compare to their differentiated counterparts. During the cell cycle, PSCs undergo symmetric self-renewal, which generates two daughter cells, each of which retains pluripotent identity. It has been shown that PSCs devote approximately 60%[15] of time to

the S phase and lack a fully formed G1 phase. Since most differentiated cell types spend the majority of their time in G1 phase, the shorter G1 phase of mESCs can account for their rapid rate of cell division[18]. By structuring the pluripotent cell cycle so that it lacks extensive gap phases and consists mainly of alternating rounds of DNA replication (during S phase) and chromosome segregation (during M), the PSCs retain its characteristic rapid self-renewal capacity. Studies have shown that most cyclins and Cdks are functionally redundant during mouse development as demonstrated by knockout studies[19-23]. The exceptions are cyclin A[24], with homozygous null mutants surviving only until 5.5 dpc and cyclin B1[25], with no homozygous null mutant survived to birth. Although the expression of the majority of cyclins has been described in PSCs, with the exception of the mitotic regulator cyclin B, all cyclins expressed in PSCs are present at significantly higher but equivalent amounts through the cell cycle[15]. This dramatically contrasts the strict, temporal-manner fluctuation of cyclin levels responsible for regulating somatic cell cycle progression. Similar, with the exception of Cdk1-cyclin B[15, 18] complexes, most Cdk are active throughout the pluripotent cell cycle, and with much higher activities compare to somatic cell types. Experiments suggest that the unusually high level of Cdk activity in PSCs can account for their rapid cell division rate since suppressing Cdk activity reduces the rate of PSCs cell division[16, 26]. Although inhibition of Cdk activity slows down the pluripotent cell cycle, it does not alter the general cell cycle structure of PSCs[16], suggesting the unusual cell cycle feature of PSCs is related more to the absence of Cdk periodicity. The lack of Cdk periodicity in PSCs also inactivates the pRb-E2F (Retinoblastoma protein and E2F transcription factor) pathway in PSCs[16]. In somatic cells, the activation of E2F target genes

is tightly linked to the temporal activation of G1 Cdks activity[27], and are crucial in establishing the full length of the G1 phase before progression to the S phase. The elevated activity of G1 Cdks in PSCs lead to hyperphosphorylation of pRb and prevent its interaction with the E2F transcription factor, eliminating the cell cycle-dependent gene expression of E2F targets[16]. Therefore, the inactivated pRb-E2F pathway may contribute to the shortened G1 phase of PSCs.

Studies have also shown that the elevated and constitutive Cdk expression is characteristic of PSCs, and as differentiation occurs[28-31], Cdk activity collapses and becomes cell cycle-dependent. Thus, there is some obvious connection between the cell cycle machinery and unique characteristics of PSCs. PSCs, defined by their capacity to indefinably self-renewal and differentiate into all three germ layers, exhibit immense potential for disease modeling and regenerative therapy. However, the effective utilization of PSCs requires an in-depth understanding of the mechanisms that establish their cellular identity. The regulation of pluripotency maintenance and fate commitment is intimately connected to the cell cycle, with the M phase being particularly critical for cells to choose between alternative fates. The M phase is the privileged window for reprogramming and rewiring the transcriptional programs[18], and several decades of investigation have tried to reveal the underlying mechanism, from the mitotic chromatin structure to the chromatin association factors that might be involved in fate maintenance.

1.1.2 The mitotic chromatin

Chromatin structure and organization changes dramatically during mitosis. It is generally accepted the chromatin conformation transforms from a cell type-specific to a universal condense organization[32-34], where major components of transcription machinery are dissociated from their interphase binding sites and new histone modifications specific for mitosis are deposited. After mitosis, chromatin returns to its uncondensed cell type-specific shape, chromatin factors and interphase specific histone modification are re-established onto the appropriate site. Despite this upheaval, the cell type-specific gene expression and epigenetic profiles exhibited by the parental cells are faithfully transmitted to the daughter cells as they enter the G1 phase. Although it has been known for a long time that the structural and physical organization, in addition to the nucleotide sequence, of the chromosomes carries important information related to multiple processes, including the gene expression regulation, and is in part specific for cellular identity, the detailed mechanism underlying the inheritance of transcriptional memory is not fully understood.

Although the folding characteristics of interphase chromatin appear to be almost completely lost during mitosis, it does not mean the condensed mitotic chromatin has no higher order organizations[32]. The prevailing model for mitotic chromosome architecture is that chromosomes fold as longitudinally compressed arrays or stochastically position consecutive chromatin loops[33]. At the level of the nucleosome, the forces on the chromatin fiber during the condensation process causes the nucleosomes to reattribute along the condensed chromatin. Together, the mitotic chromatin exhibit distinct three-dimensional organization compare to the interphase chromatin. It is known that the interphase

chromosomes are compartmentalized into topologically associated domains (TADs)[35], a contiguous chromosomal region that largely interacts with itself and is relatively insulated from its direct genomic neighbours. However, the locus-dependent and cell-type specific TADs are mostly lost in metaphase, where the chromatin displays a universal cell-type and locus invariant mitotic conformation.

Despite the condensation and extensive reorganization of chromatin during mitosis, recent studies have shown that DNA accessibility is largely maintained during mitosis[36-38]. Through DNase I sensitivity assay coupled to high-throughput sequencing (DNase-seq), certain elements, particularly the promoters, remain sensitive to DNase I digestion during mitosis. An overall mild reduction in accessibility during mitosis is found to be concentrated among a small fraction of the "peak", or narrow sites of hypersensitivity, mostly at the distal regulatory, whereas the "hotspots", or broader regions of sensitivity, are stable and unchanged through mitosis[36]. This observation suggested that large-scale, indiscriminate steric occlusion is unlikely to produce such site-specific and spatially confined changes in chromatin accessibility. Rather, *Hsiung et al.*[36] hypothesized that transcription factor binding could generate a narrow DNase peak by evicting the nucleosomes in the vicinity of the binding site, while also recruiting factors capable of spreading along and remodeling chromatin to generate the broader accessibility pattern of the DNase hotspot. During mitosis, the reduced affinity of trans-acting factors at distal regulatory elements, partly due to mitosis-specific phosphorylation, could explain the preferential loss of DNase sensitivity at DNase peaks. In contrast, patterns of generalized accessibility across hotspots, are likely attributable to mitotically stable chromatin features,

including histone modifications and DNA methylation patterns which are retained on mitotic chromatin. The maintenance of chromatin accessibility suggests there must be chromatin features that are present in interphase chromatin are also present in mitotic chromatin, keeping the promoter sites accessible during mitosis[37, 38]. Accessibility of promoter sites during mitosis also implies that the locus, although temporarily less stable bound by factors, maintain their open conformation, and are accessible for these factors upon mitotic exit. Furthermore, this locus-specific reduction in accessibility appears to be different between cell types, and thus, might play an important role in transmitting cell type-specific transcriptional memory through mitosis. Therefore, the exact mechanism that enables the maintenance of chromatin accessibility might be different for individual loci and remains largely unsolved.

1.1.3 Mitotic bookmarking as a mechanism for transmitting cell fate through mitosis

Even though most transcription activity ceases and at least a subset of proteins are dissociated from the chromosomes during mitosis, cells are capable of rearranging their chromosomes back into cell type-specific confirmation and re-establish the cell type-specific transcription patterns. This suggests that the information required to rearrange chromosomes and re-establish interphase transcriptional activity is contained in the mitotic chromatin. Group of researchers has proposed the concept of mitotic bookmarking as a potential mechanism involved in maintaining cell type-specific information through mitosis[39-42]. It is stemmed from two main observations in the late 1990s. The first is that a greater proportion of mitotic chromatin had single-stranded DNA compared to interphase

chromatin[43], and the second revealed this single-stranded nature was correlative with the expression profiles of active gene[44]. These observations suggest that there must be molecular "bookmarks" that are retained at crucial sites on the mitotic chromatin to regulate chromatin conformation and preserve the transcriptional state during mitosis. With further studies, researchers propose that mitotic bookmarks might have two distinct functions[40-41]. First, they exert a function during mitosis, including regulating chromatin conformation. Secondly, mitotic bookmarks assist the transmission of epigenetic memory by providing the daughter cells with a blueprint of what genes to turn on or off upon mitotic exit. The previously known mitotically stable epigenetic regulatory mechanisms[41, 42], including DNA methylation, mitotically stable histone variants, open chromatin confirmations at gene promoters, and mitotically retained transcription factors can be classified as subcategories of mitotic bookmarking.

Over the past decade, studies have focused on identifying mitotically retained factors that might function as a mitotic bookmark, and multiple transcription factors and chromatin regulators retained on the mitotic chromatin has been shown to play a role in mitotic bookmarking. For instance, Mixed Lineage Leukemia (MLL)[45], a histone methyltransferase, was one of the first components of the chromatin-remodeling complex identified as a mitotic bookmark. The mitotic retention of MLL was correlated with rapid transcriptional reactivation of the genes bookmarked by MLL during mitosis in HeLa cells. Later studies have revealed that the mitotic bookmarking marking activity is not limited to chromatin-modifying enzymes, multiple transcription factors including GATA1[46],

FOXA1[47], PARP1[48], ESSRB[49], SOX2[50], and KLF4[51], have been shown to act as mitotic bookmarks that facilitate a rapid transcriptional program of bookmarked genes.

In addition to affecting transcriptional kinetics, the bookmarking factor UHRF1[52] is involved in the maintenance of DNA methylation during mitosis, while OCT4 and SOX2[50] are required during M-G1 phase transition for maintenance of pluripotency. In a very recent study, the link between mitotic specific retention of SOX2[50] and the differentiation efficiency of PSCs has been investigated. As a member of the "core" transcriptional regulatory circuitry, SOX2 is strictly required for the maintenance of the pluripotent state while also playing a role in differentiation by favouring neuroectodermal commitment. Through the aid of the mitotic degradation domain (MD) of cyclin B1, which has been shown to induce mitotic specific degradation of linked proteins, *Deluz et al.*[50] demonstrated that the presence of SOX2 during the mitosis to G1 transition is required for its ability to drive neuroectodermal differentiation in mESCs. Through a similar technique, *Liu et al.*[51] showed that the mitotic specific degradation of OCT4 leads to increasing number of partially or completely different colonies in culture.

1.1.4 ChIP-MS reveals putative pluripotency-associated mitotic bookmarks

Although several factors have been successfully identified as mitotic bookmarks based on a single protein targeted approach, the present studies have not yet shown a reliable method to identify mitotic bookmarking factors at a global proteome level. In addition, the functional relevance of the genomic sites specifically bound by MBFs during mitosis in relation to pluripotency and differentiation have not been examined.

Our lab had developed a novel chromatin immunoprecipitation followed by mass spectrometry (ChIP-MS) protocol to identify factors that are retained on mitotic chromosomes in PSCs[53]. The ChIP-MS approach utilized antibodies against histone 3 (H3) or a mitotic specific histone modification, phosphorylated serine 10 on histone 3 (H3S10P) to pull down proteins associated with global chromosomes or mitotic chromatin, respectively. Immunoprecipitated proteins were subsequently identified by mass spectra analysis and *de novo* sequencing (Figure 1a). Since the normal PSC culture only contains a small fraction of mitotic cells, PSCs were enriched with nocodazole and verified using MPM2 antibody[54], which recognizes the phosphorylated version of a peptide sequence that is present in over 40 different eukaryotic proteins present at the onset of mitosis.

Peptide sequences obtained from mass spectrometry were filtered based on a series of threshold values and candidates common amongst all three biological replicates that exhibit both global (H3 fraction) and mitotic (H3S10P fraction) chromatin association were selected for follow-up (Fig 1b left)[53]. Using previously published RNA-sequencing (RNA-seq) datasets, the putative mitotic bookmarking factors were classified based on their expression level in mESCs under different culturing conditions: mESCs medium with leukemia inhibitory factor (LIF) or differentiation medium with retinoic acid (RA)[53]. Putative bookmarking factors were grouped into three categories: the RA-specific bookmarks, generic bookmarks, and pluripotency-specific bookmarks (Fig 1b right). In addition, the bookmarking factors that previously known to cause mitotic defects or DNA damage upon knockout were discarded, leaving a final list of 31 putative bookmarking factors which were validated using immunofluorescence to confirm their association with

mitotic chromosomes. Several proteins from our final list, including UTF1, DNMT3a, UHRF1, and PARP1, have previously been described to be retained on the mitotic chromatin. Amongst them, PARP1 was recently shown to be a mitotic bookmark that is associated with rapid reactivation of genes upon mitotic exit in HEK293 cells[48]. Our ChIP-MS data provided a pool of candidate mitotic bookmark that requires further study to reveal their roles in chromatin remodeling, epigenetic inheritance, and gene expression during mitosis in PSCs.

1.1.5 ATAC-seq reveals bookmarked sites during mitosis

To supplement the ChIP-MS screen, our lab has also established the chromatin accessibility profiles of PSCs in interphase (asynchronous sample), during mitosis (G2M sample), and upon mitotic exit into G1 (G1t20 sample and G1t35 sample) using the assay for transposase-accessibility chromatin followed by sequencing (ATAC-seq). The ATAC-seq assay involves treating cells with a hyperactive Tn5 transposase and DNA adapters[55]. Upon encountering a genomic site that is unprotected, Tn5 cleaves the DNA and results in the insertion of DNA adapters, which can later be sequenced to identify regions of high accessibly. We defined mitotically bookmarked site as genomic regions that maintained their chromatin accessibility state throughout mitosis into G1 (Figure 2a)[53]. Consistently with previous data, we found that majority of the sites were shared between interphase and mitotic population, and these putative bookmarked sites are mostly located within gene promoters and at the distal intergenic region. In addition, our data also suggested that while a significant portion of the genome retains the same mitotic chromatin accessibly signature,

as during interphase, there is a large percentage that losses accessibility during mitosis and early G1 phase.

Recently, *Liu et al.*[51] had shown that the H3K27Ac epigenetic mark is retained on mitotic chromatin and is highly correlated to the mitotic binding site of OCT4, SXO2, and KLF4. We examined the overlapped between our proposed putative bookmarked site identified in ATAC-seq with the mitotic specific site of H3K27Ac, as well as the known binding sites of several putative mitotic bookmarks (Figure 2b). We found a strong colocalization between H3K27Ac marks only with our putative bookmarked sites but not non-mitotically bookmarked sites identified using ATAC-seq[53]. Majority of the H3K27Ac bookmarked sites did not co-localize with any of the other mitotic bookmarks, while the two highest co-occupancy occur with KLF4 and PARP1. A comparison of expression of the genes bookmarked by H3K27Ac, KLF4, and PARP1 in differentiation vs. pluripotency condition identifies a group of genes that show higher expression in pluripotency[53], suggesting that, in addition to known pluripotent mitotic bookmarks KLF4, PARP1 is highly likely to play a role in pluripotency maintenance through mitotic bookmarking.

1.2 Functional analysis of the mitotic bookmarking capability of PARP1

1.2.1 Background

PARP1, or poly(ADP ribose) polymerase I, belongs to the poly(ADP-ribose) polymerase family[56], which are proteins catalyzes the transfer of ADP-ribosyl group from NAD^+ to various substrates. Poly(ADP-ribose) polymers (pADPr) serves as an important post-translation protein modification, and thus PARP1 play an important role in a variety of processes including DNA damage response, regulation of chromatin structure, differentiation, and transcription regulation[57]. PARP1, as a founding family member, is conserved among eukaryotes except in yeast and has the highest expression level in PSCs[56]. The structure-function relationship of PARP1 is well understood, four out of six domains have been assigned a particular function: (1) a DNA-binding domain composed of two zinc-finger structures, (2) a nuclear localization signal (NLS) domain, (3) a protein interaction domain containing BRCT motif, and (4) a catalytic domain.

The role of PARP1 in facilitating DNA repair has been clearly demonstrated by the generation of PARP1 deficient mouse model[57-60], which exhibit normal development but showed hypersensitivity to ionizing radiation and alkylating agents. Numerous studies have shown chromatin association of PARP1, and extensive binding of PARP1 makes chromatin denser and more compact[61, 62], thus preventing the transcription machinery from initiation gene transcription. *In vitro* studies confirm PARP1 ability to regulated chromatin structure, as adding recombinant PARP1 to purified chromatin changes its conformation of the chromatin from an open state to a more condensed state[62]. Meanwhile, *in vivo* studies

suggested mouse PARP1 is necessary for stable gene silencing on the inactive X chromosomes[57]. PARP1 is also shown to localize to other constitutive heterochromatin regions, including centromeres and telomeres. Due to its chromatin remodeling activity, it is not surprising that PARP1 was reported as an important factor specifically for the early stages of induced PSC reprograming[63]. *Roper et al*.[64] observed a downregulation in both PARP1 and PARP7 upon PSCs differentiation. Both PARP1 and PARP7 deficient PSCS exhibited significant downregulation of multiple pluripotency markers, including OCT4, NANOG, and SOX2. Although PARP1 deficient mice are viable and fertile, subcutaneous injection of PARP1 deficient PSCs formed cells with trophoblast giant cell-like morphology[65-67]. Further studies showed an increased propensity to differentiate into trophoblast lineage in PARP1 deficient PSCs both *in vivo* and *in vitro*. The exact mechanism underlying the ability for PARP1 to regulate pluripotency has been liked to its ability to interact with and regulates SOX2 activity[68-70]. In response to fibroblast growth factor (FGF)/extracellular signal-regulated kinase (ERK) signaling, PARP1 auto-poly ADP-ribosylation enhances SOX2-PARP1 interaction, which subsequently inhibits SOX2 binding to OCT4/SOX2 enhancers stimulating proper differentiation. In addition to the ribosylation function, *Lodhi et al.*[48] have demonstrated that PARP1 is retained at certain gene promoters in HEK293 cells through chromatin immunoprecipitation with sequencing (ChIP-seq). Using a knockdown approach, they have also demonstrated that PARP1 is important for the rapid transcriptional reaction of its mitotic target genes in early G1 phase, confirming its role as a mitotic bookmarking factor in HEK293.

1.2.2 Summary of Intent

Since PARP1 is identified as a putative mitotic bookmark in PSCs from our ChIP-MS screen[53], and its mitotic occupancy exhibit extensive overlap with the genomic locus bookmarked by H3K27Ac[53], it represented a suitable pilot study to examine the mitotic bookmarking function of PARP1 within the context of PSCs. The first part of my research project aimed to explore the mitotic bookmarking function of PARP1 in relation to its ability to maintain pluripotent identity in PSCs. Our research was carried out using E14Tg2a mESCs due to their robust self-renewal capacity. Based on the evidence in previous studies, we *hypothesized that the presence of PARP1 on mitotic chromatin is necessary for optimal self-renewal in pluripotent stem cells*. The following research aims were formulated to help test our hypothesis:

Aim 1: Generate and characterize PARP1 knockout PSCs

Aim 2: Evaluate the effect of mitotic-specific loss of PARP1 on the self-renewal of PSCs

Aim 1 was addressed by generating and selecting PARP1 knockout PSCs using CRISPR/Cas9 technique to completely ablate the DNA binding activity of PARP1. The confirmed PARP1 knockout clones were utilized to exploit the effect of PARP1 deficient on cell cycle progress, proliferation, self-renewal capacity, and gene expression pattern. In addition, the chromatin interaction dynamic of PARP1 during mitosis and interphase were compared using fluorescence loss in photobleaching (FLIP).

Aim 2 was addressed by using recombinant Parp1 construct fused with a mitotic degradation domain from Cyclin B, which is previously employed by multiple groups to

study the functional relevance of mitotic bookmarks in cell fate decisions. PARP1 rescue lines with PARP1 expression selectively eliminated from specific phases of the cell cycle were generated by introducing wild-type Parp1 or MD-fusion constructs into the PARP1 knockout clones characterized in Aim 1. The self-renewal capacity of each PARP1 rescue lines was then explored to reveal the effect of mitotic specific perturbation of PARP1 on cell fate.

Together, this study was designed as a systematic survey of the functional relevance mitotic bookmarking activity of PARP1 in PSCs. It compressively examined how the chromatin association of PARP1 is related to pluripotency, how the PARP1-chromatin interaction dynamic changes from interphase to mitosis, and what are the phenotypic outcomes of perturbing PARP1 chromatin association during M-G1 transition.

1.2.3 Material and methods

Cell culture: E14TG2A mouse embryonic stem cells were cultured on 0.1% gelatin-coated culture dishes in mESC media: DMEM (Sigma Aldrich, D5796), 15% FBS, 1X non-essential amino acids (Life technologies: 11140-050), 1X glutamax (Life technologies: 35050-061), 1X sodium pyruvate (Life technologies: 11360-070), and 1X betamercaptoethanol (Gibco: 21985-023). Media was further supplemented with 1000 U/mL LIF (Amsbio, AMS-263-100) after filter-sterilization with a 0.22μm filter (Sigma) Cells were maintained at 37ºC, 5% CO_2 and passage every three days using accutase® (Sigma Aldrich: A6964). PARP1 knockout cells were routinely maintained on a layer of x-ray irradiated mouse embryonic fibroblasts (xMEFs) seeded at a density of $1x10^6$ cells/60 cm^2. mESCs were pre-plated on gelatin-coated dishes for 30 minutes to deplete xMEFs.

Cell proliferation assay: $1X10^5$ mESCs/well, were seeded in 24-well plates and cultured for 48 hrs. The cells were then trypsinized into single cell suspension using accutase® (Sigma Aldrich: A6964) and automatically counted using the Automated Cell Counter Countess II (ThermoFisher). To avoid quantification of xMEFs, mESCs were pre-plated on gelatin-coated dishes for 30 minutes to deplete xMEFs. Proliferation rates or cell doubling time (DT) was calculated using the following formulate: $DT = \frac{(t-t_0)log2}{logN-logN_0}$, where t, t_0 indicate time points at counting and initial plating, respectively; and N, N_0 indicate the number of cells at respective time points. Results are presented as mean doubling time ± SD of 5 consecutive passages.

Colony initiation cell assay: mESCs were seeded at a density of 250 cells/well onto a well of a 12-well plate with x-MEFs at a density of $1x10^6$ cells/plate. For each experiment, cells were seeded in a technical triplicate and cultured for 5 days. At day 5, colonies were fixed in the dish with 250 ul of 4% PFA (Electron microscopy sciences, Cat # 15710) for 1-2minutes and washed with water. Alkaline phosphatase (AP) staining was performed as described in Sigma AP staining kit (86R-1KT, Sigma). Plates were scanned on EPSON Scanner with 3200 dpi and 24-bit colour and analyzed on ImageJ (Schneider et al., 2012). Dense colonies with intense AP staining were characterized as AP positive (AP+) while the less dense ones with dispersed pink staining around the edges were characterized as mixed colonies.

Fluorescence loss in photobleaching (FLIP): FLIP experiments were performed on Leica SP5 confocal microscopy at McMaster Biophotonics Facility. mESCs with stable PARP1-mKO2 expression was imaged and bleached using a 561-nm laser. To reduce background fluorescence, the cell culture medium was exchanged before imaging for mESC media made with DMEM lacking phenol red (Gibco^{TM}). In mitotic cells, we measured time traces of average fluorescence from a square region in the area containing condensed chromosomes while continuously bleaching another region containing condensed chromosomes within the same cell. In interphase cells, both bleaching and measurement regions were inside the nucleus.

Flow cytometry: Cell cycle profiles were established by fixing cells at various time points using the BD fixation and permeabilization kit (Cat # 554714). The fixation solution was diluted with 3 parts PBS to achieve a final paraformaldehyde (PFA) concentration of 1%, and cells were fixed for 10minutes at room temperature. Cells were Hoechst (Life technologies: H1399) for DNA and MPM2 (05-368, Millipore) as a mitotic marker. Donkey anti-mouse Alexa Fluor 647 (Thermo Fisher A-31571) was used as a secondary antibody. Samples were acquired on the MACSQuant® analyzer (Milteny Biotech), and analyzed using FlowJo.

Generation of PARP1 knockout: PARP1 knockout mouse ES lines were generated by using guide RNAs again exon 2 of mouse Parp1 gene. Guide RNAs were designed using Benchling and cloned into CRISPR/Cas9 backbone, pSpCas9(BB)-2APuro (PX459) V2.0 (a gift from Feng Zhang (Addgene plasmid # 62988)) (Ran et al., 2013). 10 ug of the cloned CRISPR/Cas9 plasmid was used to transfect a well of 6-well plate of wild-type ES cells (p6). Cells were selected with 2ug/ml of Puromycin for 72 hours and colonies were allowed to form. Individual colonies were hand-picked and screen by western blot with the anti-PARP1 antibody (Abcam ab194586). Positive clones were amplified around the targeted region using genomic DNA primers (Table 1) and sequenced using Sanger sequencing.

Mitotic degron construct: The DNA sequence encoding the peptide corresponding to residues 13-91 of murine cyclin B1 (Kadauke et al.) was subcloned into pCAG-mKO2 using MD primers (Table 1) to generate the mitotic degron construct (MD). The MD and

inactive mutant MD^{R42A} (Kadauke et al.) were fused to the C-terminus of pCAG-PARP1-mKO2 to create pCAG-PARP1-mKO2-MD and pCAG-PARP1-mKO2-MD^{R42A}.

Mitotic enrichment and release: WT and PARP1KO mESCs were seeded at a density of 2.5M per T75 0.1% gelatin-coated tissue culture flasks. Each flask was supplemented with 0.5M x-ray irradiated MEFs (mouse embryonic fibroblasts). mESCs were enriched using a double thymidine and nocodazole block (Teves et al. 2016). Mitotic cells were collected by mitotic shake off and were released (M-released) into regular mESC media after washing off nocodazole (1X with PBS) for 20mins at 37C. M-released cells (G1t20) were kept cold from this point on and were resuspended in PBS with 2%BSA, 5mM EDTA and 7AAD (BD 559925 at 1:100). A fraction of G1t20 cells were washed and resuspended gently in mESC media and release back into G1 at 37^{o}C for 15mins. Cells were then collected for G1t35. Collected cells from each fraction (Interphase, G2M, G1t20, and G1t35) were cryopreserved in 15% FBS and 10% DMSO.

qRT-PCR: RNA was isolated using TrizolTM LS (Thermo Fisher 10296028) according to manufacturer's protocols. For nascent RNA q-RT-PCR, RNA was DNaseI treated in solution and purified using Qiagen RNeasy Micro Kit (Qiagen Cat # 74004). cDNA was prepared for 1ug of RNA using SensiFAST cDNA Synthesis Kit (Froggabio BIO-65054), and q-PCR was performed using SensiFAST SYBR No-ROX Kit (Froggabio CSA-01194). Primers were designed to capture nascent transcripts (Table 2) CFX ManagerTM was used to analyze the data (Biorad, Software #1845000).

Statistical analysis: All statistical analyses were performed using Prism 7 (GraphPad) and Microsoft Excel software. Error bars reflect the standard error of the mean unless otherwise stated. The paired two-tailed Student's t-test was used to compute all p-values in cell tracking experiments for comparison of the intensities under distinct channels for individually tracked cells; all other p-values were computed with the unpaired two-tailed student's t-test. Unless otherwise stated error bars represent standard error of the mean and alpha of 0.05 was used as a cut-off for statistical significance.

Western blot: Single-cell suspensions harvested during the passage of mESC cultures were lysed in 1X radioimmunoprecipitation assay buffer (RIPA, Sigma) with 1X Protease Inhibitor Cocktail (Roche). The protein concentrations were quantified using the DC Protein Assay kit (Biorad) with the bovine serum albumin standard curve ranging from 0 to 2 mg/ml concentrations. The quantified protein extracts were transferred into 1X NuPAGE LDS Sample Buffer (Thermo Fisher) with 15% Bond-Breaker TM TCEP Solution (Thermo Fisher). The prepared extracts were heated at 95^{o}C for 5 minutes and separated on a 12% polyacrylamide gel at 180V for 45 minutes. The separated protein was transferred onto a PVDF membrane using constant-current electrophoresis at 200 mA for 2 hours, followed by blocking in 5% milk in 1X TBS. The proteins were then blotted with monoclonal antibodies (Table 3) in 3% milk in 1X Tris-buffered saline (TBS) containing 0.1 % Tween20 (1X TBST; Bio Shop) at 4^{o}C overnight. After washing, the blot was incubated with the secondary anti-rabbit HRP-conjugated antibody (1:20,000; Biorad) in 3% milk in 1X TBST for 1 hour at RT and was developed for 10 minutes using an HRP

substrate (1:5 diluted in ultrapure water; Lumina). The blot was visualized using the ChemiDoc™ MP Imaging System (BioRad) with its associated ImageLab analysis software (Biorad).

1.2.4 Results and Discussions

Knocking out PARP1 did not affect the cell cycle progress and proliferation rate of mESCs

Using CRISPR/Cas9, we generated PARP1 knockout mESC lines by disrupting exon 2 within the DNA-binding domain of PARP1 (Figure 3a). Two clones of PARP1 knockout mESC lines were selected, where PARP1KO8 had independent mutations in both the alleles and PARP1KO24 had a homozygous mutation (Figure 3b). In both cases, the open reading frame of PARP1 was disrupted and lead to a complete loss of detection of protein product (Figure 3c).

The initiation characterization of PARP1 knockout lines involved quantifying the growth rate and cell cycle profile of selected knockouts. Our data showed that both PARP1 knockouts and wild-type mESCs had a doubling time of 16-18 hours (Figure 4a), suggesting the proliferation rate of mESCs was not significantly affected by knockout out PARP1. Moreover, using Hoechst and MPM-2 antibodies, we were able to quantify the percentage of mESCs in different stages of the cell cycle (Figure 4b). Since the cell cycle profile of asynchronous PARP1 knockouts was unchanged compared to wild-type ES cells, we concluded that the association of PARP1 with mitotic chromatin was not involved regulation of cell cycle progression.

The transcript level of pluripotency-related genes remained unchanged in the stable PARP1 knockout

Roper et al.[64] have previously reported that in the PARP1 deficient mESCs exhibit a decrease in ground state pluripotency and a higher propensity to differentiate, as they

display a significant reduction in transcript level of *Nanog* and *Stella* but significant increase in transcript level of *Cdx2*. To examine the transcription profile, RT-qPCR was carried out on genes previously shown to change in expression by knocking out PARP1. Surprisingly, we initially observed a significant decrease in the transcript level of *Stella* in the PARP1 knockout (Figure 5a), but it was eventually returned to a similar level as the wild-type control over 12 passages (Figure 5b). Based on the RT-qPCR results in later passages, the transcript level of all gene tested did not exhibit significant changes between the knockout and the wild-type controls. The inconsistent results we obtained compare to *Roper et al.* might be related to the different techniques used to generate PARP1 knockouts. Roper et al. obtained the PARP1 knockout line from *Wang et al.*[71], who originally inactivated *Parp1* gene in mESC through homologous recombination, inserting a PGK-neo cassette in exon 4 of the *Parp1*. Successfully targeted mESCs were injected into mouse blastocysts to generated heterozygous mice, which were then intercrossed to produce homozygous mouse completely devoid of PARP1 expression. Since their PARP1 knockout mESCs were isolated from the PARP1 null mice, there might be the inherent difference from our knockout lines, which were directly generated via non-homologous end joining from the wild-type mESC targeting the second exon of *Parp1*.

Moreover, there are also previous reports that suggest compensation of lost PARP1 activity from PARP2 might occur in PARP1 stable knockout[69]. PARP2 is discovered as a result of the presence of residual DNA-dependent PARP activity in embryonic fibroblasts derived from PARP1 deficient mice[72]. PARP2 exhibits strong structure resemblance in its catalytic domain with PARP1 but a slightly different DNA-binding domain. Studies have

shown that PARP2 interacts with PARP1 and shares common partners involved in DNA repair and chromatin structure[73]. PARP2 deficient mouse displays phenotypes both similar to PARP1 deficient mouse and unique to PARP2 deficiency, indicating that PARP1 and PARP2 functions are complementary but do not fully overlap. Mice with PARP1 and PARP2 double knockout are not viable and die at the onset of gastrulation but not with either single knockout suggest that PARP1 and PARP2 might compensate each other for its lost function, and the presence of either PARP1 and PARP2 are sufficient for normal embryonic development. *Lai et al.*[69] have shown that in PSCs, PARP2 was upregulated in PARP1-depleted cells and PARP1 was upregulated in PARP2-depleted cells, suggesting a reciprocal compensation between PARP1 and PARP2 in PSCs (Figure 6). Contradictory to other reports, they also found that the stable knockdown of PARP1 and PARP2 resulted in slightly different gene expression pattern comparing to transient knockdown, where the expression of *Nanog* and *Klf4* become less significantly upregulated. Additionally, *Ogino et al*[74] have also reported that changes in the expression of pluripotency genes are minimal in PARP1 knockout cells. The differences in gene expression pattern observed between stable PARP1 knockouts or knockdowns and transient PARP1 knockdowns suggest there might be a time-dependent transcription feedback loops in PSCs that gradually adjust expression of pluripotency-related genes to the normal levels.

Transcriptional reactivation profile of PARP1 targets was mostly unchanged in PARP1 knockouts

To examine the gene transcription profiles of PARP1 target genes upon mitotic exit, we utilized a mitotic enrichment protocol consisting of a double thymidine block followed by a nocodazole treatment[75] (Figure 7a top). The mitotic cells (t0) were collected by mitotic shake-off and release into G1 for 20 minutes, 35 minutes, and 45 minutes. We also collected G2 fraction that remained adherent after mitotic shake-off. The cell cycle profile of each collected samples was confirmed by flow cytometry (Figure 7a bottom). We quantified the nascent RNA transcript level of PARP1 targets[70] that were also differentially accessible by our ATAC-seq data[53] using RT-qPCR. Although minimal differences were observed in the result, the mitotically enriched PARP1 targets, *Eda2r* and *Kdm6a*, seemed to be slightly upregulated in mid- to late-G1 phase for knockout compare to wild-type control (Figure 7b), suggesting PARP1 may be acting as a repressor for these genes upon mitotic exit into G1 for maintaining normal PSCs expression profile.

Due to experimental constraints, we were only able to measure a very small fraction of the total PARP1 bookmarked sites, and further characterization of other PARP1 targets are required before ruling out the role of PARP1 in assisting transcript reactivation upon mitotic exit. Additionally, recent studies suggest that mitotic bookmarks may have additional functions other than rapidly re-establish transcription activity during M-G1 transition. For instance, SOX2[50], mitotic bookmarks crucial for maintaining pluripotency, does not seem to alter its target gene transcription upon mitotic exit. Since the small population of PARP1 targets tested was insufficient to represent the phenotypical definition

of pluripotency, we decided to directly test the self-renewal capacity of PARP1 knockout using colony initiation cell (CIC) assay.

Knocking out PARP1 significantly reduced the self-renewal capability of PSCs

The CIC assay utilizes alkaline phosphatase (AP)[76] staining which has been shown to specifically recognize undifferentiated populations within a culture. Overall, knocking out PARP1 significantly decreased the number of AP-positive colonies formed compared to the WT controls (Figure 8), suggesting a possible role of PARP1 in pluripotency maintenance. Since CIC assay was able to provide us with a consistent and evident phenotypical measure of self-renewal, we decided to use CIC assay as a primary approach for test whether abrogation of PARP1 during M-G1 transition would impair pluripotency.

PARP1 displayed distinct mobility on mitotic chromosomes

To examine the dynamics of PARP1 chromatin association, we performed fluorescence loss in photobleaching (FLIP) experiment, which mainly reflects interactions with the nonspecific binding site. The wild-type and PARP1 knockout were transfected with the *Parp1-mKO2* expression construct and FLIP was conducted on both the interphase and mitotic mESC populations to quantify the mobility of PARP1 at different stages of the cell cycle. Overall, we observed a slower fluorescence loss in mitosis comparing with the interphase for both wild-type and knockout lines (Figure 9), suggesting PARP1 are exchanged less between mitotic chromosomes and the mitotic cytoplasm than within the interphase nucleus. This lower exchange rate might be due to a stronger affinity of

molecules bound to mitotic chromosomes, revealing PARP1 might exhibit a differential chromatin interaction during mitosis comparing to interphase. *Deluz et al.*[50] have observed a similar reduction in mobility during mitosis comparing to interphase with SOX2, suggesting this enhanced mitotic chromatin binding affinity might be one of the characteristics of mitotic bookmarks.

Presence of PARP1 during M-G1 phase transition was required for optimal self-renew

Previous studies have shown that PSCs do not display the distinct oscillation of phase-specific cyclin-dependent kinases normally observed in differentiated cell types, except the mitotic regulatory Cdk1-cyclin B[25]. The Cdk1-cyclin B activity in PSCs is highly correlated with mitosis where it increases at the onset of mitosis and declines rapidly when PSCs enter the G1 phase. Based on this observation, *Kadauke et al.*[42] have fused the mitotic degradation domain (MD) of cyclin B1 to the coding sequencing of GATA1, which has successfully induced the mitotic specific degradation of GATA1 during the metaphase-anaphase transition. Later, *Deluz et al.*[50] have adopted this approach to examine the role SOX2 plays during the M-G1 transition.

Using a similar approach, we generated MD construct by fusing the MD and an inactive MD (MD^{R42A}) at the 3' end of the *Parp1* coding sequence. Together with the wild-type *Parp1* construct, they were transfected into both wild-type and PARP1 knockout to generated rescue lines (Figure 10a). Combining with the previously established CIC assay, we were able to examine the self-renewal of each rescue lines. From the result, both the wild-type *Parp1* and *Parp1-*MD^{R42A} constructs were able to restore the self-renewal of KO

to an optimal level similar to the wild-type control, but the *Parp1-MD* construct failed to do so (Figure 10b). This result confirmed our hypothesis that the presence of PARP1 on mitotic chromatin is necessary for optimal self-renewal in pluripotent stem cells. In addition, we also observed a significant reduction in colony sizes with PARP1 knockouts, however, this reduction was not rescued by any Parp1 constructs we have tested (Figure 10c). The inability for wild-type Parp1 constructs to rescue the reduced size of PARP1 knockout colonies suggesting that cells lacking PARP1 might develop irreversible damages that cannot be compensated by other PARP proteins or rescued by re-introducing PARP1. Whether this irreversible damage is related to PARP1 mitotic bookmarking ability cannot be confirmed in our assay, and further study is necessary to reveal the link between colony size and pluripotent identity.

1.2.5 Conclusions

The aim of this project was to develop a systematic approach to examine the functional relevance mitotic bookmarking activity of PARP1 in PSCs. To that end, we first examined the effect of knocking out PARP1 on the pluripotent state. Although several studies have reported changes in transcript level of pluripotency marks in PARP knockouts, the results are not consistent depending on the method used to generate PARP1 knock and the length of time the cells are depleted of PARP1. Similar results were observed in our study, where the transcript level of *Stella* was initially downregulated but returned to a level comparable to wild-type control in later passages of PARP1 knockout. Whether this adjustment in transcript level in the stable PARP1 knockout is due to PARP2 compensation or other selective pressure in PSCs is beyond our scope of the study. However, to examine the pluripotent state beyond the level of transcript expression, we showed that knockout out PARP1 did reduce self-renewal in PSCs using CIC assay without affect proliferation and cell cycle progression. In addition, using the FLIP experiment, we showed that a significantly reduced mobility of PARP1 bound to mitotic chromosomes compare to interphase chromosomes suggesting PARP1 may exhibit higher affinity for nonspecific sequences on nucleosomal DNA.

To investigated the mitotic bookmarking role of PARP1, we initially used the traditional approach by checking the transcriptional reactivation profile of PARP1 target[70] upon mitotic release in PARP1 knockout and wild-type controls. Although *Eda2r* and *Kdm6a* seemed to be slightly upregulated in mid- to later-G1 in PARP1 knockout, minimal differences were observed in most PARP1 targets. It is worth mentioning that the targets

we tested represent only a very limited fraction of the total sites bookmarked by PARP1, and further characterization of other gene loci are required to make a statistically relevant conclusion on the ability of PARP1 to regulated transcription reactivation. As an attempt to study the bookmarking function of PARP1 on fate decision, we assayed the effects of rescuing PARP1 knockouts with a modified PARP1 protein (PARP1-MD) that will be degraded during the M-G1 phase transition. Our results showed both wild-type PARP1 and inactive PARP1-MD^{R24A} were able to rescue the colony forming defects observed in PARP1 knockouts, but knockout rescued with PARP1-MD retained the reduce self-renewal confirmed that the presence of PARP1 during M-G1 phase transition was essential for the optimal self-renewal of PSCs.

In conclusion, using PARP1 as a model, we demonstrated an effective approach for examining the phenotypic effects of perturbation of mitotic bookmarks during late mitosis. In the next section, we would be confirming that this approach can be adapted to study other putative mitotic bookmarks identified by our ChIP-MS screen by examining the mitotic bookmarking role of HDGF and PSIP1 in PSCs.

1.3 Assaying the mitotic bookmarking capability of PWWP domain-containing factors

1.3.1 Background

To follow up on our model developed with PARP1, we decided to focus on a group of factor identified from our ChIP-MS data that contain the PWWP domain. The PWWP domain containing proteins serves a particular interest, as they have been previously shown to exhibit dual function, binding both DNA and methlysine histones[77-79]. The PWWP domain is named for its conserved Proline-Tryptophan-Tryptophan-Proline motif, and structural analysis revealed the PWWP domain forms a prominent positively charged surface rich in lysine and arginine, suggesting a potential role in DNA binding. Several groups have revealed that residues potentially involved in DNA binding are centered on the patch of highly positively charged surface[77], suggesting the PWWP domain interacts with the phosphate backbone of DNA through electrostatic interaction and thus lacking sequence specificity. On the other hand, the structural similarity between the PWWP domain and other Royal superfamily members[80], which can recognize methylated lysine and arginine, signifying the PWWP domain might also interact with histones. *In vitro* studies demonstrated that multiple PWWP domain-containing proteins, including DNMT3a and HDGF2[77], preferentially bind to di- and tri-methylated lysine on histones.

We identified two PWWP domain-containing proteins from our list of putative mitotic bookmarks, the hepatoma-derived growth factor (HDGF)[77] and PC4 and SFRS1 interacting protein (PSIP1)[78]. Due to the high sequence homology between their PWWP domains, HDGF and PSIP1 are categories into the HDGF subfamily. Members of this subfamily share a highly

conserved N-terminal region containing the PWWP domain that preferentially interacts with H3K36me3, H3K79me3 and H4K20me3[77]. Both proteins are expressed in a wide range of cell types and have been identified as having a number of putative roles. HDGF is a nuclear protein with mitogenic and heparin binding activity[81-83]. It is highly expressed in developing heart and fetal gut, and as a growth factor[84-87], HDGF has been implicated in organ development and tissue differentiation of the intestine, kidney, liver, and cardiovascular system. Generation of mice from HDGF deficient ES cells suggests HDGF is dispensable in mouse development as mice are viable with no phenotypic abnormalities, and fibroblasts isolated from the HDGF knockout mice revealed no alteration in proliferation and cell cycle distributions[84]. Interaction studies reveal that the PWWP domain is indispensable for HDGF interactions including both protein-protein and protein-DNA interaction[77]. In addition, gene expression profiling analysis showed that HDGF was predominately a transcriptional repressor, by modulating chromatin structure and acting together with transcriptional corepressors[86]. As an HDGF-related protein (HRP)[78], PSIP1 has been extensively studied and implicated in transcriptional regulation of stress-related genes, alternative splicing, DNA repair, and integration of HIV into the host genome[88-93]. PSIP1 encodes two protein isoforms, p52 and p75 which differ in expression among tissues[78, 89, 93]. Generation of mice deficient for PSIP1 revealed homeotic skeletal transformations[92, 93], consistent with those observed in mice missing various *Hox* genes. Transcriptional profiling of PSIP1 deficient cells revealed no significant changes in *Hox* gene expression in mouse embryonic fibroblasts but did demonstrate dysregulation of these genes in human embryonic kidney cells, suggesting dysregulation of *Hox* genes by the loss of PSIP1 is lineage specific.

1.3.2 Summary of Intent

Although HDGF and PSIP1 have been studied extensively regarding their function in various tissue, they have not yet been examined in relation to their mitotic bookmarking function. Since both factors were found to be strongly associated with the mitotic chromatin, we would like to characterize their role in maintaining the cellular identity of PSCs through mitotic bookmarking. Based on our observation with PARP1, *we hypothesize that HDGF and PSIP1 are retained on a subset of its interphase binding site during mitosis, and the presence of HDGF or PSIP1 on mitotic chromatin is necessary for optimal self-renewal in pluripotent stem cells*. The following research aims were formulated to help test our hypothesis:

Aim 1: Characterize the self-renewal of HDGF and PSIP1 knockouts, and evaluate the effect of mitosis-specific loss of HDGF and PSIP1 on the self-renewal of pluripotent stem cells

Aim 2: Identify the global interphase and mitotic chromatin-specific binding sites of HDGF and PSIP1

Aim 1 was addressed by adopting the methodology we developed for studying the mitotic bookmarking capability of PARP1, which induced the mitotic specific degradation of the protein of interest in PSCs and examined the changes in self-renewal using CIC assay.

Aim 2 was addressed by performing ChIP following by high-throughput sequencing on interphase and mitotic population to identify the genomic loci that are bookmarked by HDGF and PSIP1 during mitosis. Since it has been previously reported that paraformaldehyde (PFA) fixation might lead to exclusion of mitotic bookmarks from the mitotic binding site with weak binding affinity, we decided to conduct ChIP-seq experiment

using both fixed and native cells to ensure an unbiased capture of HDGF and PSIP1 associated sites.

Together, this study was designed to confirm the methodology we have developed with PARP1 can be applied to study other mitotic bookmarks in PSCs in terms of their ability to regulate self-renewal. In addition, through comparative analysis using the ATAC-seq datasets generated previously by our lab, we would like to obtain a better understanding of the relationship between the mitotic assessable sites and genomic regions bookmarked by different factors.

1.3.3 Material and methods

Cell culture: E14TG2A mouse embryonic stem cells were cultured on 0.1% gelatin-coated culture dishes in mESC media: DMEM (Sigma Aldrich, D5796), 15% FBS, 1X non-essential amino acids (Life technologies: 11140-050), 1X glutamax (Life technologies: 35050-061), 1X sodium pyruvate (Life technologies: 11360-070), and 1X betamercaptoethanol (Gibco: 21985-023). Media was further supplemented with 1000 U/mL LIF (Amsbio, AMS-263-100) after filter-sterilization with a 0.22μm filter (Sigma) Cells were maintained at 37ºC, 5% CO_2 and passage every three days using accutase® (Sigma Aldrich: A6964). PARP1 knockout cells were routinely maintained on a layer of x-ray irradiated mouse embryonic fibroblasts (xMEFs) seeded at a density of $1x10^6$ cells/60 cm^2. mESCs were pre-plated on gelatin-coated dishes for 30 minutes to deplete xMEFs.

Cross-linked chromatin immunoprecipitation: $1x10^7$ mESCs were used per IP with $1ug/1x10^7$ cells of antibody. Cells were cross-linked in 1% paraformaldehyde (PFA) for 10 minutes at room temperature with shaking and then washed 2X in large volumes of PBS. Cross-linked cells were lysed in RIPA buffer (50mM Tris-Cl pH7.45, 50mM NaCl, 0.1%SDS, 2%NP-40, 1% Sodium deoxycholate) supplemented with protease inhibitors (11836153001 cOmpleteTM mini-tablets Roche, Sigma) for 30 at 4ºC. Nuclear and chromatin pellet was collected by gentle centrifugation at 2500 g for 5min at 4C. The pellet was resuspended in RIPA dilution buffer (RDB, 50mM Tris-Cl pH7.45, 150mM NaCl) and supplemented with protease inhibitors, and homogenized with an 18G needle. The lysate

was gently sonicated to release shearing chromatin (6 pulses each with 20s ON, 30s OFF at 30% amplitude). Sheared chromatin supernatant was collected by spinning at 10,000 g for 10 min at 4^{o}C. Chromatin was diluted in RDB to get a final SDS concentration of 0.025% to assist in IP. The samples were reverse cross-linked at 95^{o}C for 10 min, and run on a precast 10% bis-tris gel (Cat# NP0322, ThermoFisher) following the western blot protocol.

Colony initiation cell assay: mESCs were seeded at a density of 250 cells/well onto a well of a 12-well plate with x-MEFs at a density of 1x10^{6} cells/plate. For each experiment, cells were seeded in a technical triplicate and cultured for 5 days. At day 5, colonies were fixed in the dish with 250 ul of 4% PFA (Electron microscopy sciences, Cat # 15710) for 1-2minutes and washed with water. Alkaline phosphatase (AP) staining was performed as described in Sigma AP staining kit (86R-1KT, Sigma). Plates were scanned on EPSON Scanner with 3200 dpi and 24-bit colour and analyzed on ImageJ (Schneider et al., 2012). Dense colonies with intense AP staining were characterized as AP positive (AP+) while the less dense ones with dispersed pink staining around the edges were characterized as mixed colonies.

Flow cytometry: Cell cycle profiles were established by fixing cells at various time points using the BD fixation and permeabilization kit (Cat # 554714). The fixation solution was diluted with 3 parts PBS to achieve a final paraformaldehyde (PFA) concentration of 1%, and cells were fixed for 10minutes at room temperature. Cells were Hoechst (Life technologies: H1399) for DNA and MPM2 (05-368, Millipore) as a mitotic marker.

Donkey anti-mouse Alexa Fluor 647 (Thermo Fisher A-31571) was used as a secondary antibody. Samples were acquired on the MACSQuant® analyzer (Milteny Biotech) and analyzed using FlowJo.

Mitotic degron constructs: The DNA sequence encoding the peptide corresponding to residues 13-91 of murine cyclin B1 (Kadauke et al.) was subcloned into pCAG-mKO2 using MD primers (Table 1) to generate the mitotic degron construct (MD). The (MD) and inactive mutant MD^{R42A} (Kadauke et al.) were fused to the C-terminus of pCAG-HDGF-mKO2 and pCAG-PSIP1-mKO2 to create MD and MD^{R24A} construct.

Statistical analysis: All statistical analyses were performed using Prism 7 (GraphPad) and Microsoft Excel software. Error bars reflect the standard error of the mean, unless otherwise stated. The paired two-tailed Student's t-test was used to compute all p-values in cell tracking experiments for comparison of the intensities under distinct channels for individually tracked cells; all other p-values were computed with the unpaired two-tailed student's t-test. Unless otherwise stated error bars represent standard error of the mean and alpha of 0.05 was used as a cut-off for statistical significance.

Western blot: Single-cell suspensions harvested during passage of mESC cultures were lysed in 1X radioimmunoprecipitation assay buffer (RIPA, Sigma) with 1X Protease Inhibitor Cocktail (Roche). The protein concentrations were quantified using the DC Protein Assay kit (Biorad) with the bovine serum albumin standard curve ranging from 0

to 2 mg/ml concentrations. The quantified protein extracts were transferred into 1X NuPAGE LDS Sample Buffer (Thermo Fisher) with 15% Bond-Breaker TM TCEP Solution (Thermo Fisher). The prepared extracts were heated at 95^{o}C for 5 minutes and separated on a 12% polyacrylamide gel at 180V for 45 minutes. The separated protein was transferred onto a PVDF membrane using constant-current electrophoresis at 200 mA for 2 hours, followed by blocking in 5% milk in 1X TBS. The proteins were then blotted with monoclonal antibodies (Table 3) in 3% milk in 1X Tris-buffered saline (TBS) containing 0.1 % Tween20 (1X TBST; Bio Shop) at 4^{o}C overnight. After washing, the blot was incubated with the secondary anti-rabbit HRP-conjugated antibody (1:20,000; Biorad) in 3% milk in 1X TBST for 1 hour at RT and was developedped for 10 minutes using an HRP substrate (1:5 diluted in ultrapure water; Lumina). The blot was visualized using the ChemiDoc™ MP Imaging System (BioRad) with its associated ImageLab analysis software (Biorad).

1.3.4 Results and Discussions

HDGF and PSIP1 knockout PSCs displayed reduced self-renewal

Using CRISPR/Cas9, we generated HDGF and PSIP1 knockout mESC lines by disrupting exon 1 of HDGF and exon 3 of PSIP1, located within the PWWP domain. The loss of expression of HDGF and PSIP1 was confirmed by western blot (Figure 11a). Morphologically, our knockout cell lines were identical to wild-type, consistent with what is described in the literature. Although previous studies have shown that the proliferation and cell-cycle profile were not altered in fibroblast isolated from HDGF and PSIP1 deficient mice[84, 92], none has examined changes in pluripotent state. As both HDGF and PSIP1 were classified as generic mitotic bookmarks based on RNA-seq data, we need to determine whether ablation of HDGF and PSIP has influenced pluripotency. Therefore, CIC assay was used to test the self-renewal of HDGF and PSIP1 knockouts. We observed a significant reduction in AP-positive colonies form with both HDGF or PSIP1 knockouts compare to the WT control (Figure 11b), suggesting HDGF and PSIP1 do play a role in regulating pluripotency.

Mitotic specific degradation of HDGF did not alter the self-renewal of PSCs

Since we confirmed that knocking out HDGF negatively affected the self-renewal of PSCs, we next tested whether the absence of HDGF during M-G1 transition was responsible for this observation. Adopting the approach developed from studying PARP1 in part 1, we generated rescue constructs where the coding sequence of Hdgf where either fused with MD or MD^{R42A}. The wild-type and HDGF knockouts were rescued using the wild-type Hdgf, Hdgf-MD, or Hdgf-MD^{R42A} constructs, and western blot was performed to ensure each rescue line was expressing the correct construct (Figure 12a). The CIC assay performed on rescue lines

suggested that the presence of HDGF during M-G1 transition was not essential for optimal self-renewal, as the number of AP-positive colonies formed in all rescue condition was not significantly different compared to the wild-type control (Figure 12b). Therefore, the reduced self-renewal observed with HDGF knockout might not be directly related to the mitotic bookmarking activity of HDGF. It is possible that the reduced self-renewal is more connected with the growth factor characteristic of HDGF[82-86], as it is a complex protein with multiple roles in different cell types. To our surprise, we also observed a significant difference between the numbers of AP-positive colonies form in HDGF knockouts when we initially set up CIC assay (Figure 11b) comparing to the rescue experiment (Figure 12b). The defective self-renewal capability originally observed with HDGF knockouts seemed to be slowly returning to wild-type level, although the rescue experiments still resulted in a significant difference between the HDGF knockout and the wild-type controls. Our observation was somewhat consistent with previously reports, which suggest that the HDGF knockdown but not HDGF stable knockout exhibit a reduced proliferation[84], signifying there might be long-term adaptive compensation from other HRP. In addition, studies have shown HDGF is released from necrotic cells, signaling cell and tissue damage, suggesting HDGF acts as a trophic factor or signaling molecules only under abnormal conditions. Therefore, our results does not necessarily suggest HDGF does not function as a mitotic bookmark in PSCs as CIC assay only test a specific aspect of pluripotency, the self-renewal capability. It is important to note that the ability for PSCs to differentiate into various tissues cannot be accessed simply from CIC assay.

Identifying the global interphase and mitotic chromatin-specific binding sites of HDGF and PSIP1

Very limited number of studies have examined the DNA binding activity of HDGF and PSIP1, and studies have yet described DNA-binding profile of HDGF and PSIP1 in PSCs. Therefore, it is important for us to sequence the genomic loci that are bound HDGF and PSIP1 during interphase and mitosis to identify regions they bookmarked during mitosis. To address the previously reported artifacts associated with PFA fixation[75], we could compare the efficiency of cross-linked ChIP and native ChIP for identifying sites bound by HDGF and PSIP1. Based on previous experience and an initial experiment, we derived a sonication parameter that produces DNA fragments ranging from 300-500 bp (Figure 13a). The pull-down efficiency for antibody against HDGF or PSIP1 was tested using ChIP followed by western blot (Figure 13b). The results showed clean bands at expected size for both PSIP1 and HDGF, and there were very minimum protein present in the supernatant or unbound fraction, confirm the specificity and high efficiency for HDGF and PSIP1 antibodies for ChIP experiment.

1.3.5 Conclusion and future directions

Supplementing the missing gaps in the field of mitotic bookmarking, we generated a list of putative mitotic bookmarks that have not yet been fully explored in the context of their bookmarking role. Using PARP1 as a model, we demonstrated an effective approach to examine the mitotic bookmarking activity of molecular bookmarks in pluripotency maintenance, and this approach can be applied to examine other factors that are retained on the mitotic chromatin, as shown with the HDGF and PSIP1 example. However, there are several experiments need to be completed before any conclusion can be drawn for the mitotic bookmarking activity of HDGF and PSIP1. Due to cloning issues, there is a delay in PSIP1 rescue experiment and we are currently generating the rescue lines with stable expression of wild-type Psip1, Psip1-MD, or Psip1-MD^{R24A} construct. After confirming the expression of each rescue lines, CIC assay will be performed to test the mitotic bookmarking role of PSIP1 in self-renewal. Meanwhile, the pull-down efficiency needs to be examined in native ChIP using non-crosslinked cells. After successfully establishing the optimal condition for cross-linked and native ChIP, we will perform a preliminary test of HDGF and PSIP1 chromatin association using know HDGF and PSIP1 targets, including *Smyd1*[94] and *HoxA*[93] genes. The official ChIP-seq sample would be prepared using mitotic enrichment protocol and optimized pull-down condition. Once we have obtained the ChIP-seq data, we will be able to use comparative bioinformatics to identify sites that are differentially bound during mitosis compare to interphase. Combining with the ATAC-seq data[53] and previously published ChIP-seq data of known mitotic bookmarks, we can further

characterize the identified bookmarked sites that do not co-related with the binding site of currently know mitotic bookmarks.

There are several questions that have raised from our data. With regarding both PARP1 and HDGF, differences have been observed with short-term knockdown and long-term knockout suggesting these factors are not necessary for embryonic development and adaptive compensation mechanisms do exist in mammalian cells. Therefore, it is possible that there is redundancy in mitotic bookmarks as multiple factors might be involved in bookmarking the same genomic loci. In addition, there might be the long-term effect of losing specific groups of mitotic bookmarks as the cell differentiation towards specific lineages, which cannot be tested using CIC assay or single differentiation assays. Moreover, the exact relationship between mitotic bookmarked sites, the transcription reactive profiles of bookmarked genes, and the transmission of cellular identity remain largely unexplored. It is a challenging gap to address as most mitotic bookmarks function in a non-sequence specific manner when interacting with the mitotic chromatin and a massive number of genomic regions are occupied by various factors during mitosis. Perhaps more advanced techniques that allow for highly sensitive and specific RNA sequencing over multiple developmental lineages can help link the transcriptional profile with the long-term mitotic bookmarking activities.

1.4 Figures and tables

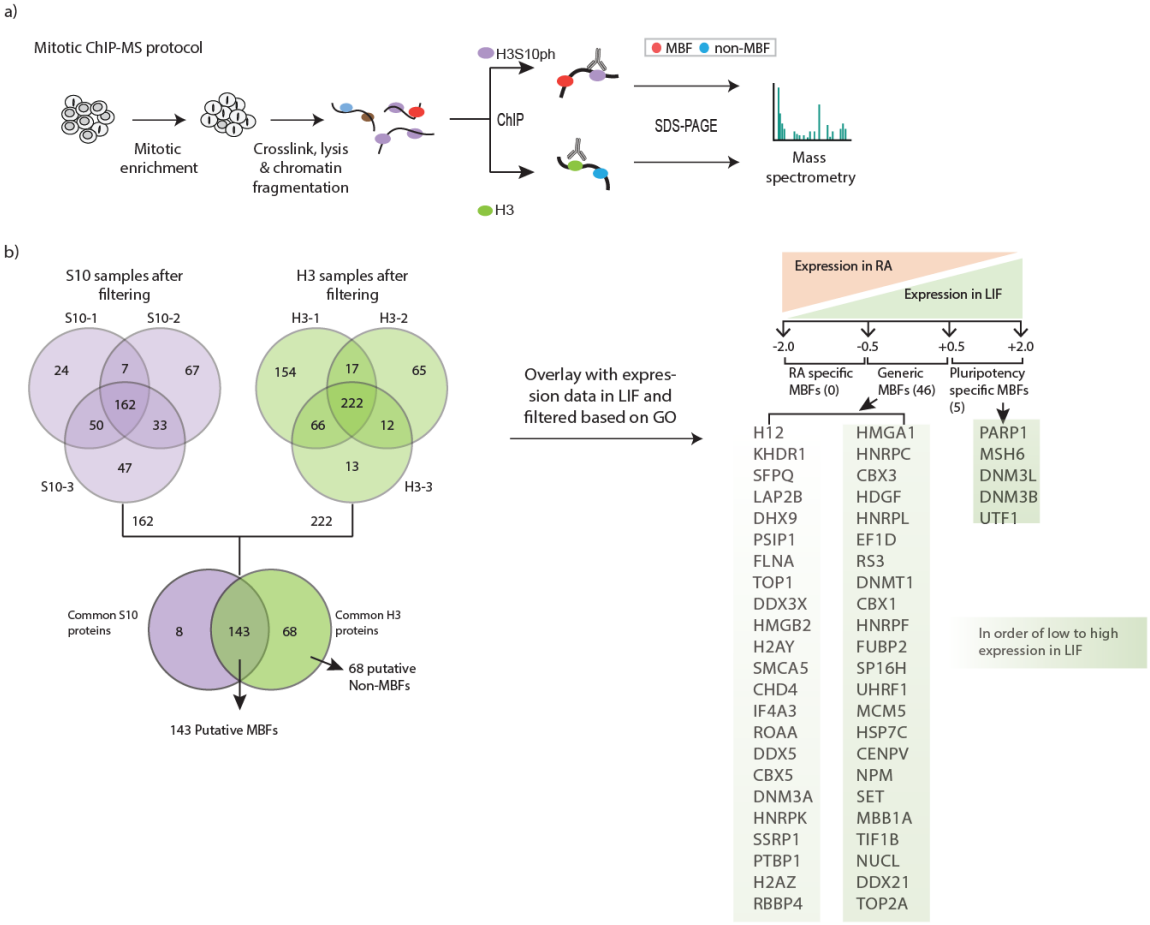

Figure 1. Identification of putative mitotic bookmarking factors from ChIP-MS data. a) The strategy used to identify putative mitotic bookmarks from the ChIP-MS screen. b) The classification of mitotic bookmarks based on their expression level in pluripotent conditions. (Figure adapted from Sonam Bhatia)

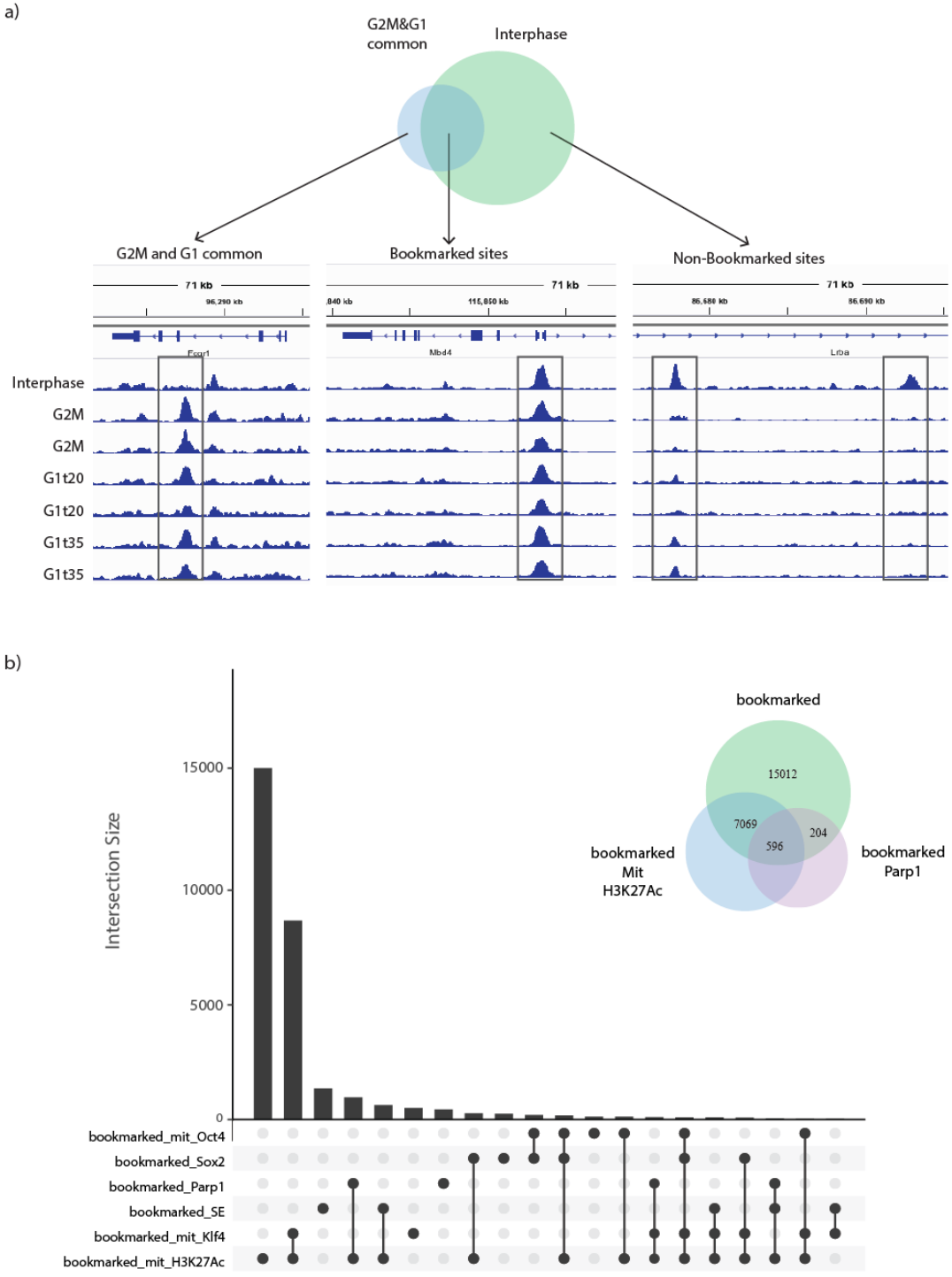
a)
G2M&G1 common
Interphase
G2M and G1 common
Bookmarked sites
Non-Bookmarked sites
71 kb
Interphase
G2M
G2M
G1t20
G1t20
G1t35
G1t35
b)
Intersection Size
15000
10000
5000
0
bookmarked_mit_Oct4
bookmarked_Sox2
bookmarked_Parp1
bookmarked_SE
bookmarked_mit_Klf4
bookmarked_mit_H3K27Ac
bookmarked
15012
7069
204
596
bookmarked Mit H3K27Ac
bookmarked Parp1

Figure 2. ATAC-seq reveals putatively bookmarked gene loci. a) Venn diagram (top) and representative signal track (bottom) showing the sites common between G2M, G1t20 and G1t25 (G2M&G1 common) and interphase, identifying the bookmarked and nonbookmarked site. B) UpSet plot showing the relationship between occupancy of bookmarked sites with the mitotic specific binding of key pluripotency-related factors, an epigenetic modification associated bookmarked sites, and a hit identified in ChIP-MS screen. Filled circles represent the overlap between the different datasets. Set size indicates the total size of the data set. The inset Venn diagram shows the extensive overlap between mitotic PARP1 binding, bookmarked site, and mitotic H3K27Ac occupancy. (Figure adapted from Sonam Bhatia)

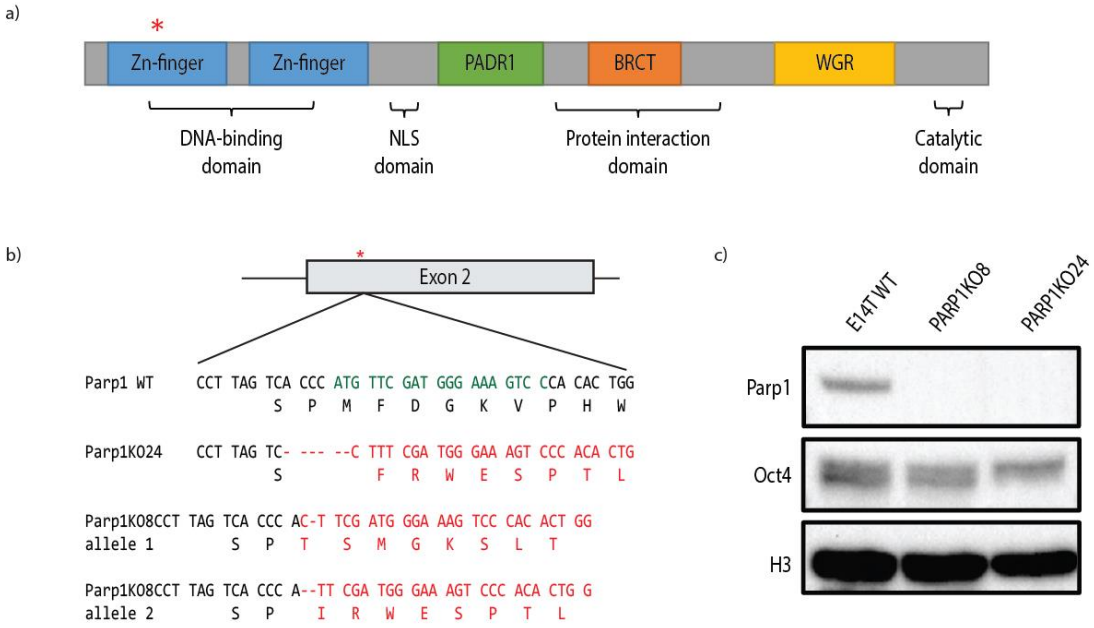

Figure 3. Generation and characterization of PARP1 knockout mouse ES lines. a) Protein structure mmParp1 (not to scale). b) The genomic sequence of the wild-type and two PARP1 knockout clones generated. Red arrow diagrammatically represents the site targeting by CRISPR/Cas9. Sequences highlined in green correspond to the binding site for guide RNA. c) Western blot showing the protein expression of PARP1, OCT4 and loading control histone H3 in WT and PARP1 knockout lines. (Figure generated using Illustrator)

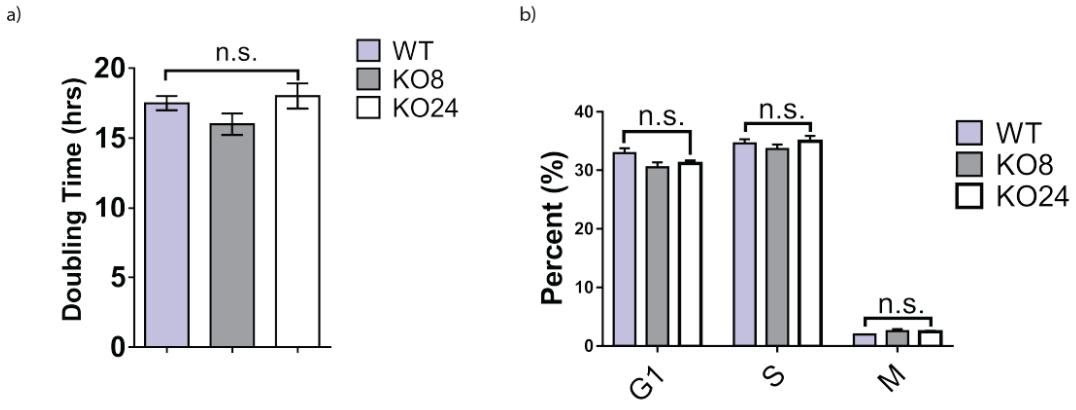

Figure 4. Proliferation rate and cell cycle profile for PARP1 knockouts. a) Proliferation rate, or the doubling time (DT), was calculated using biological triplicates (n=3). Results are plotted using mean doubling time of four consecutive passages with standard error. b) Flow experiment was performed using biological triplicates (n=3), and the average percentage of mESCs in each stage of cell cycles was plotted with standard error. (Figure generated using FlowJo and GraphPad)

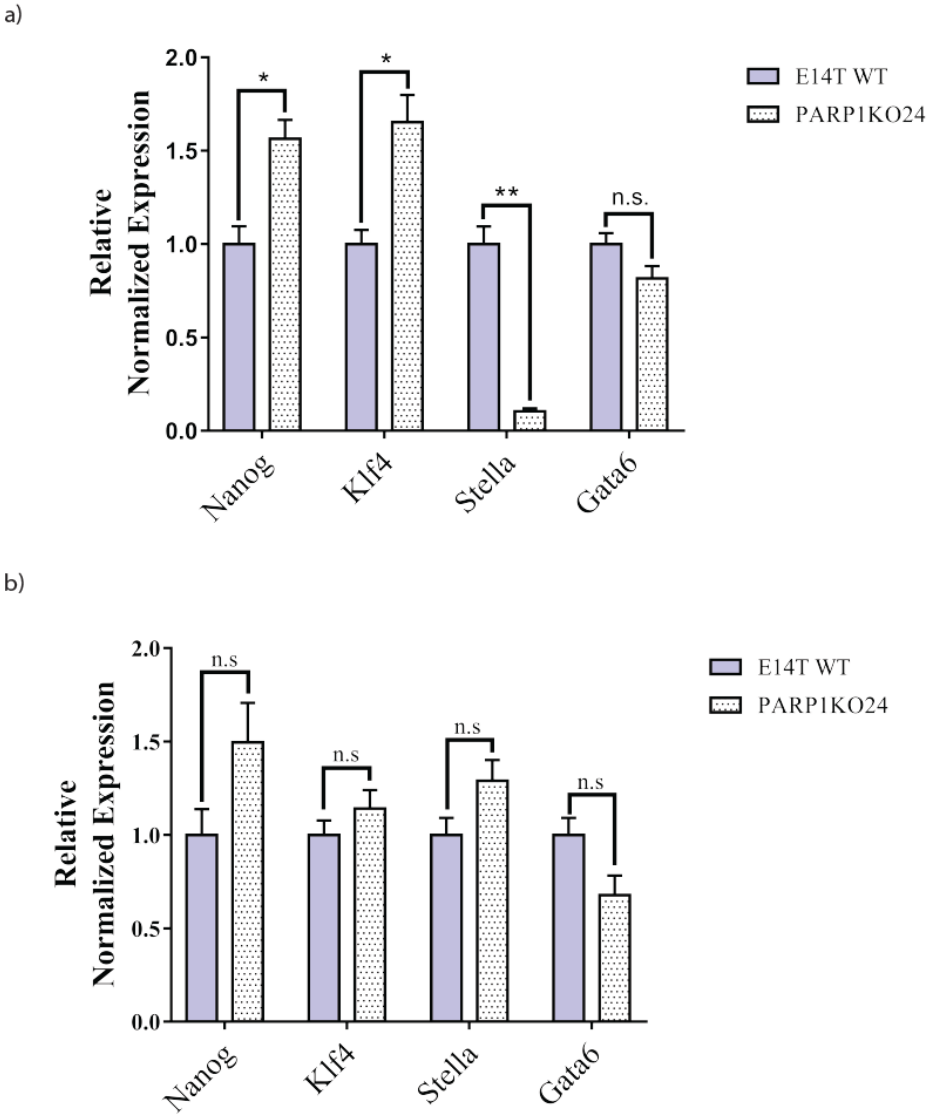

Figure 5. RT-qPCR analysis on pluripotency-related genes. Housekeeping genes, Rpl13a and Tbp, were to control for a baseline. Biological replicates (n=3) with three technical replicates per biological replicate were plotted with a standard error of the mean. a) An experiment carried out on KO lines at passage 18-20. B) An experiment carried out on KO lines at passage 30-32. Statistically significant as assessed by multiple t-tests, * $p < 0.01$, ** $p < 0.001$. (Figure generated using GraphPad)

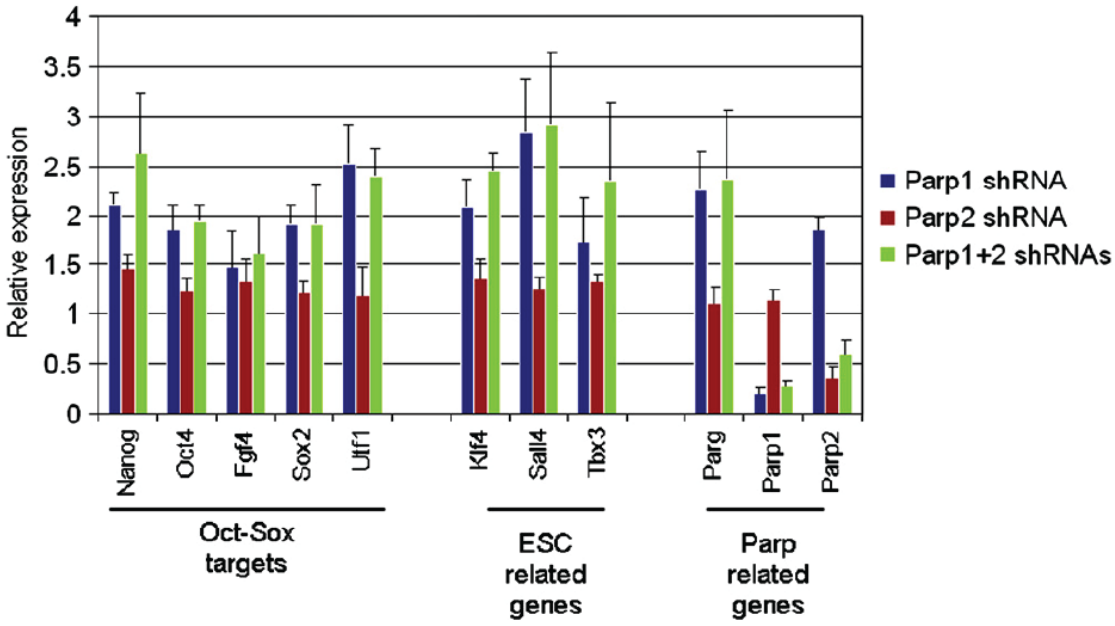

Figure 6. Transient knockdown of PARP1 and PARP2 repress OCT-SOX targets. PARP2 was upregulated in PARP1-depleted cells and PARP1 was upregulated in PARP2-depleted cells, suggesting a reciprocal compensation between PARP1 and PARP2 in PSCs. Expression levels are shown relative to the control shRNA. All mean values for experimental vs. control samples were significant at $p < 0.05$. (Figure adapted from Ref. 69)

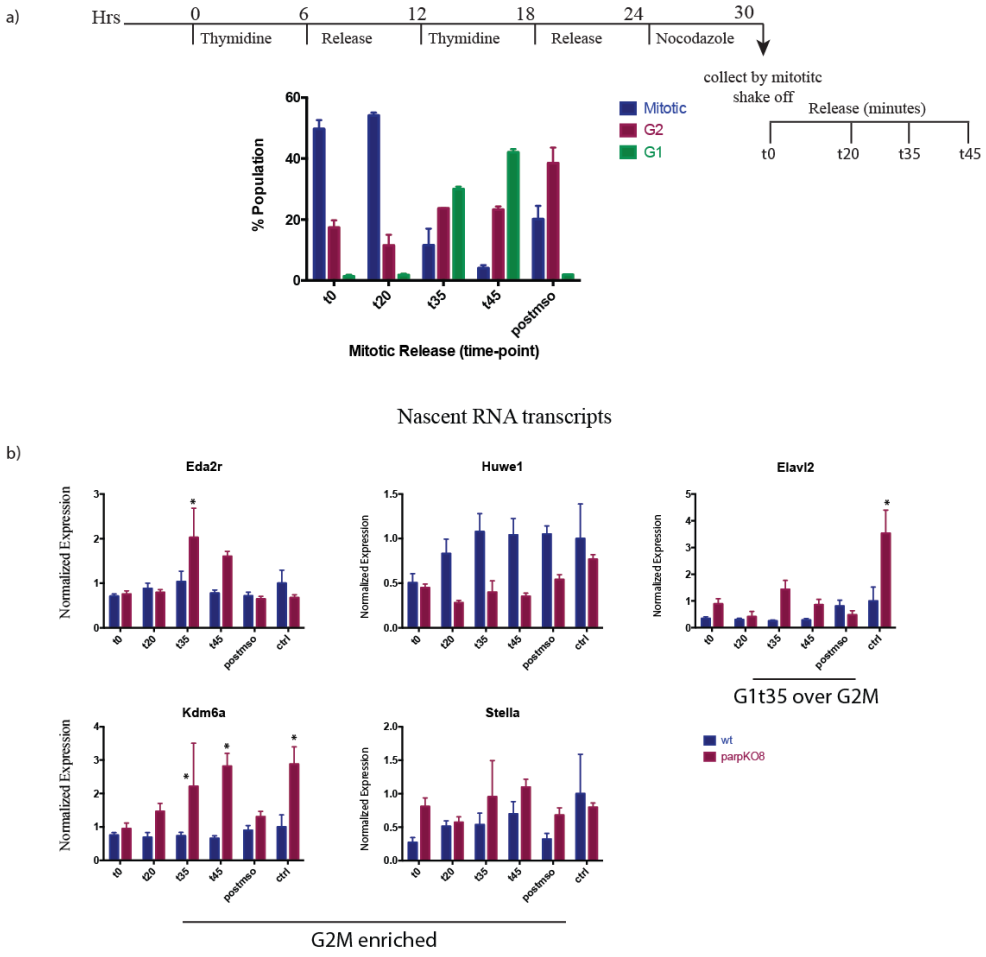

Figure 7. Transcriptional profile of PARP1 targets upon mitotic exit in WT and PARP1KO8. a) Mitotic enrichment protocol containing a double thymidine block followed by a single nocodazole treatment. Mitotically shack-off cells are released for 20 minutes, 35 minutes, and 45 minutes. Flow experiments are used to confirm the cell cycle profile of each collected sample. b) RT-qPCR of RNA transcripts of mitotic enriched (Eda2r, Huwe1, Kdm6a, Stella) and late G1 enriched (Elavl2) gene loci. Gene expression was normalized using Rpl13a and Tbp as reference genes. * Statistically significant as

assessed by multiple t-tests (alpha=0.05) (n=3 for wt and n=2 for ParpKO8). (Figure adapted from Sonam Bhatia)

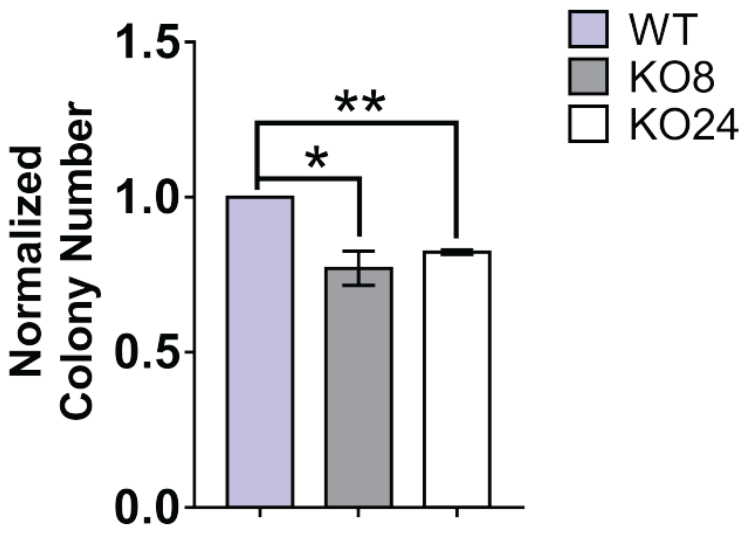

Figure 8. Self-renewal capacity of PARP1KO CIC assay. A number of colonies formed by wild-type mESCs and PARP1KOs normalized over the colonies formed in WT control. Biological replicates (n=3) with three technical replicates per biological replicate were plotted with a standard error of the mean. Statistically significant as assessed by multiple t-tests, * $p < 0.05$, ** $p < 0.005$. (Figure generated using GraphPad)

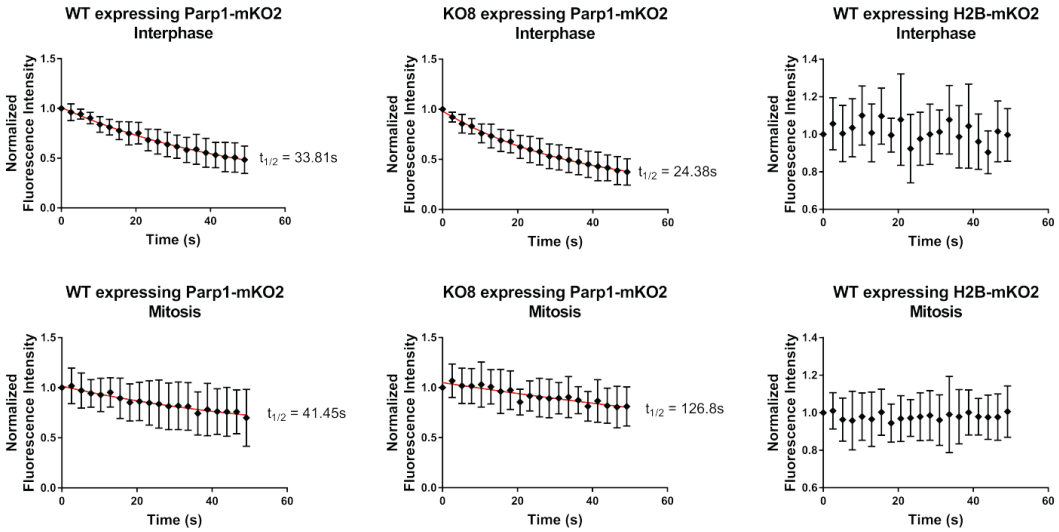

Figure 9. Dynamics of PARP1 in mitotic and interphase cells. FLIP curves (arbitrary units) for WT and PARP1KO8 expressing Parp1-mKO2 vector in interphase (top) and mitosis (bottom). H2B is an immobilized histone protein serves as a negative control. Error bar indicates a standard error, n_{min} = 20. Half-time (t1/2) is calculated based on nonlinear regression using one phase exponential decay equation. (Figure generated using GraphPad)

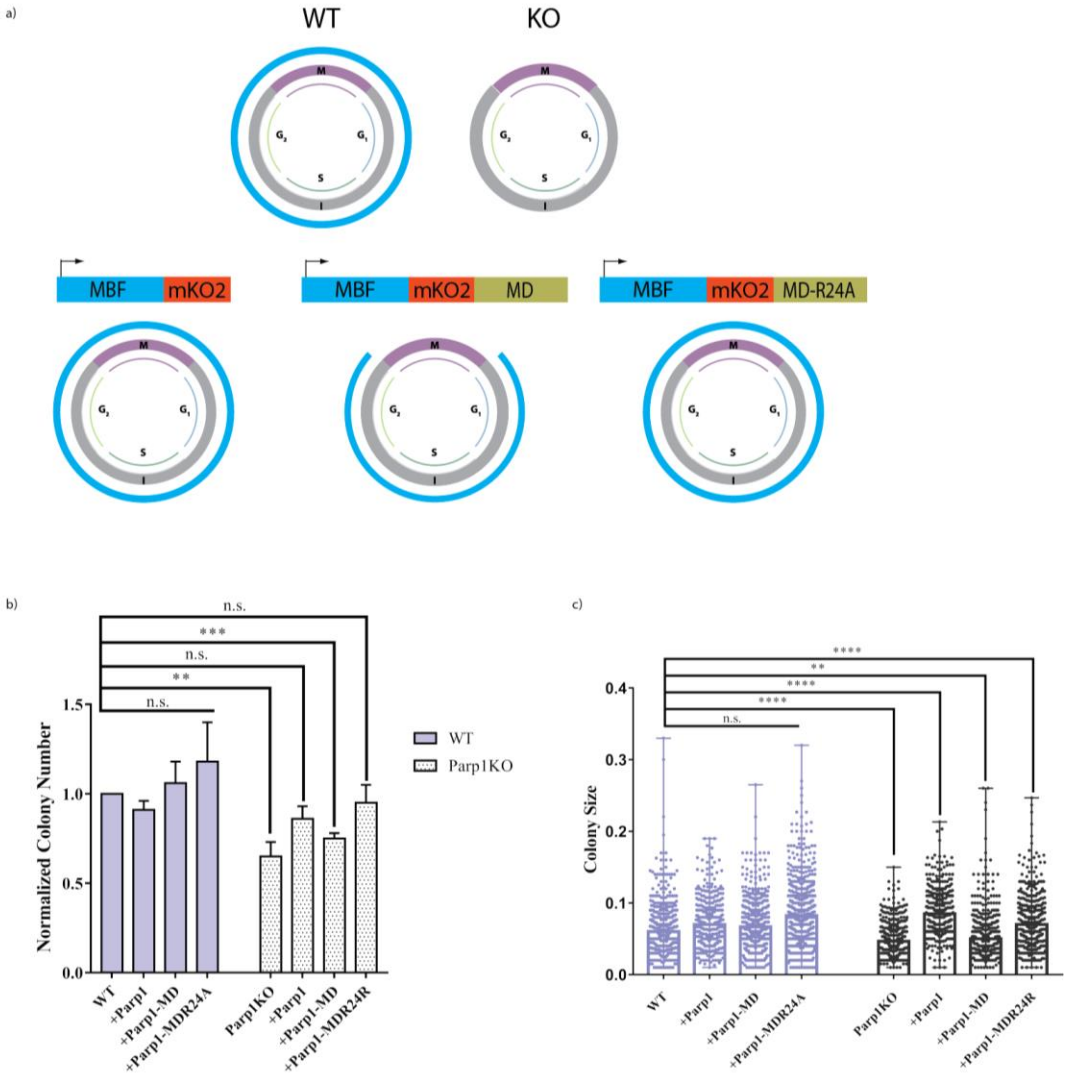

Figure 10. Phenotypic effects of perturbation of PARP1 during late mitosis. a) Schematic denoting the Parp1 expression during cell cycle for each rescue condition. b) A number of colonies obtain from CIC assay in each condition. Counts were normalized to the wild-type control. c) Colony area measured by pixel size from CIC assay. Error bars indicate SE, statistically significant as assessed by multiple t-tests, ** $p < 0.005$, *** $p < 0.0005$, **** $p < 0.0001$. (Figure generated using Illustrate and GraphPad)

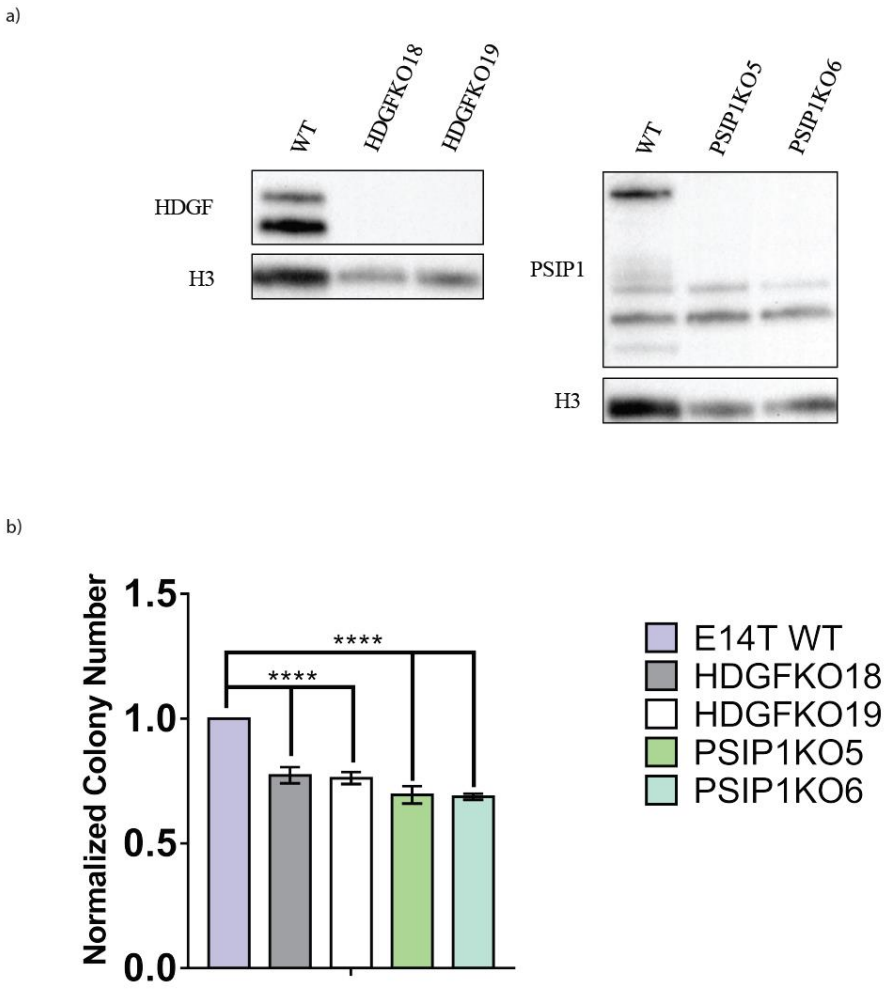

Figure 11. Characterization of HDGF and PSIP1 knockout lines. a) Western blot showing the protein expression of HDGF or PSIP1 and loading control histone H3 in WT and HDGF and PSIP1 knockout lines. b) Number of colonies formed by wild-type mESCs and HDGF and PSIP1 knockouts normalized over the colonies formed in WT control. Biological replicates (n=3) with three technical replicates per biological replicate were plotted with a standard error of the mean. Statistically significant as assessed by multiple t-tests, **** $p < 0.0001$. (Figure generated using Illustrator and GraphPad)

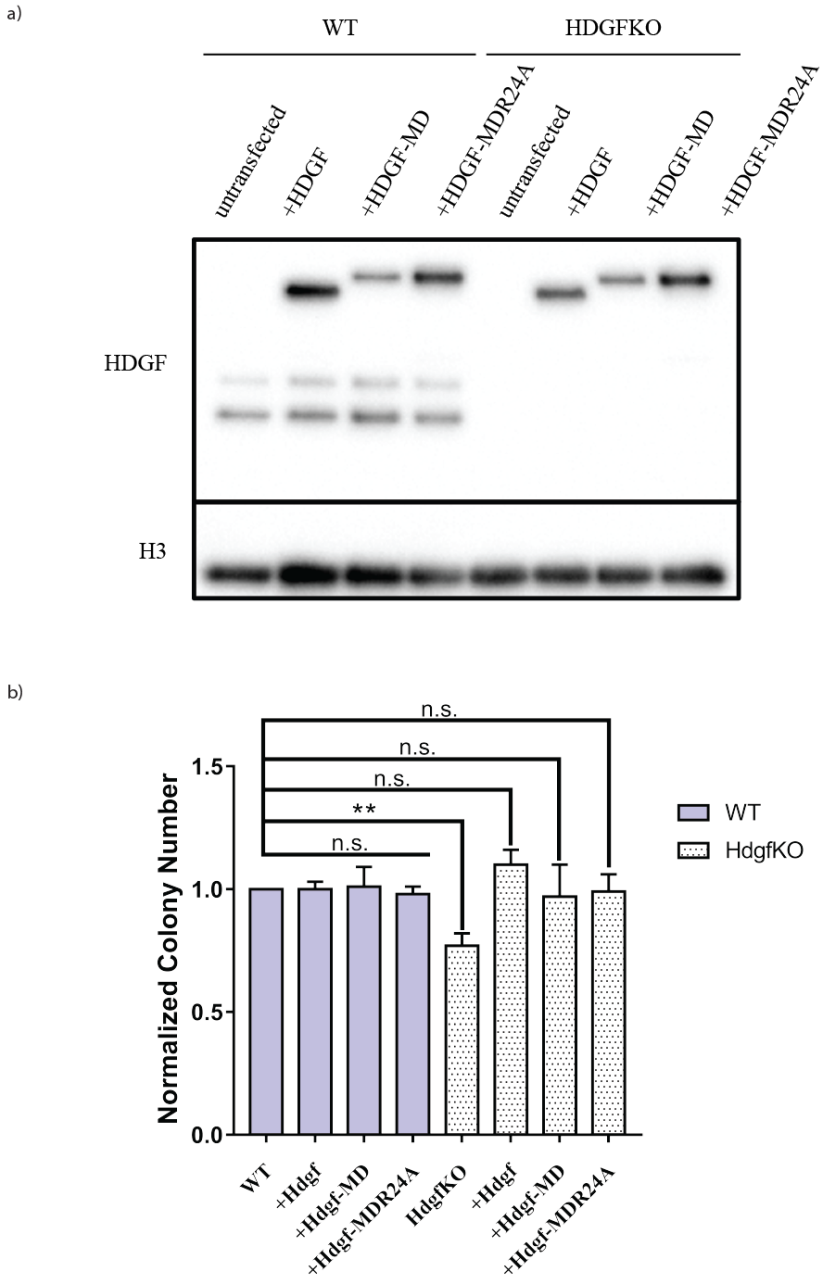

Figure 12. Phenotypic effects of perturbation of HDGF during late mitosis. a) Western blot showing the expression of Hdgf constructs in WT and KO cells. b) A number of colonies obtain from CIC assay in each condition. Counts were normalized to the wild-type

control. Error bars indicate SE, statistically significant as assessed by multiple t-tests, ** $p < 0.005$. (Figure generated using Illustrate and GraphPad)

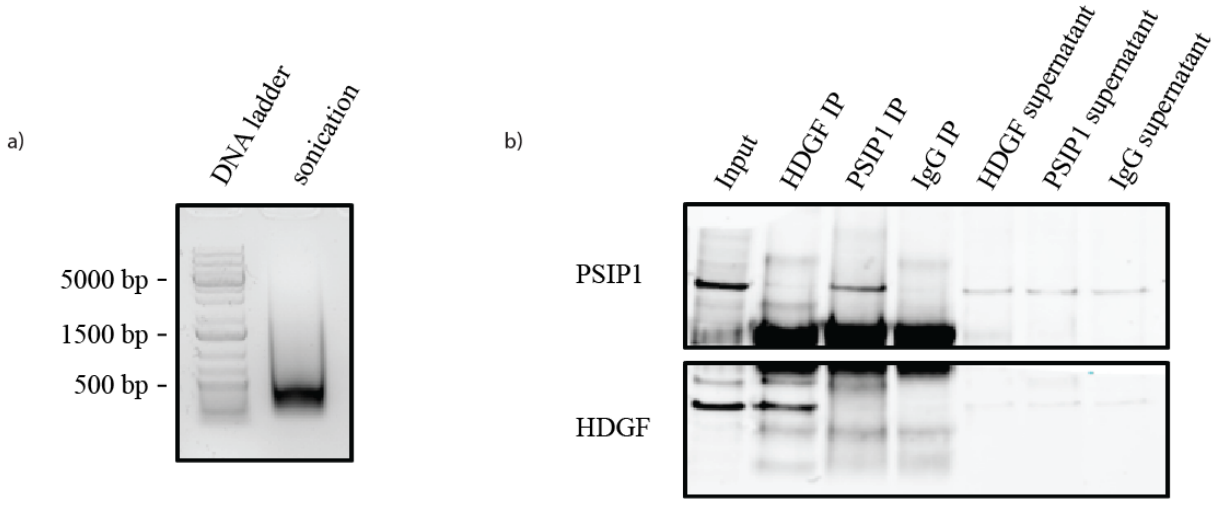

Figure 13. Optimization of cross-linked ChIP. a) Agarose gel showing the shearing of sonicated cell lysate. b) Western blot from the immunoprecipitation probed for HDGF and PSIP1. HDGF IP = anti-HDGF, PSIP1 IP = anti-PSIP1, IgG = anti-immunoglobulin G, supernatant = unbound flow-through fraction. (Figure generated using Illustrate)

Table 1: Primers used for sequencing genomic DNA of PARP1 knockout and generating MD and MD^{R24A} constructs

Name	Sequence (5'→3')	Note
CrsprParp1_gRNA-F	CACCGGGACTTTCCCATCGAACAT	sgRNA for CRISPR/Cas9 mediate KO
CrsprParp1_gRNA-R	aaacATGTTCGATGGGAAAGTCCC	sgRNA for CRISPR/Cas9 mediate KO
CrsChk_Parp1_Int1_F2	CCAGGATGAGAAGCCAGAAG	Checking genomic Parp1 DNA
CrsChk_Parp1_Exn2_R2	CAGAAGCAACTCAGCAGATAGA	Checking genomic Parp1 DNA
Age1-mKO2_F	GTACCGGTCATGGTGAGTGTGATT	MD fusion
Not1-MD_R	ATATAGCGGCCGCTTAGAATTGTG GTTCGCACACAGG	MD fusion

Table 2: Primers used for qRT-PCR, evaluating the nascent transcript levels

Gene target	Forward primer (5'→3')	Reverse Primer (5'→3')
Rpl13a	GTCACTGCCTGGTACTTCC	TCCCTCCACCCTATGACAAG
Tbp	AAGAGAGCCACGGACAACTG	AGCCCAACTTCTGCACAACT
Nanog	TGATTTGTGGGCCTGAAGAAA	GAGGCATCTCAGCAGAAGACA
Klf4	GAGTTCCTCACGCCAACG	CGGGAAGGGAGAAGACACT
Stella	CTTTGTTGTCGGTGCTGAAAG	GCTGGAGTTGCTCTTAGGTC
Gata6	GCGGGCTCTACAGCAAGATG	ACAGTTGGCACAGGACAATCC
Huwe1	ATGATGAGCAACTCCTCTTGG	GCATGTTCCCTATCCTCTGTTAT
Eda2r	CACCTATTGTGAGAGCGGTATG	CATTCGAGTACAGAGCAGACAC
Elavl2	CACAGTATGGGCGCATCATTA	TCAGTCAGGGAGCACAAGA
Kdm6a	AGACCTAGTCCTCAGATCATACC	ATCGTCAAACACTTCACTCTGT

Table 3: List of antibody used for western blot and immunoprecipitation

Target	Source	Identifier
PARP1	Abcam	ab6079
OCT4	BD Biosciences	BD611203
HDGF	Abcam	ab128921
PSIP1	Abcam	A300-847A
H3	Millipore	06-570

1.5 References

1. Evans, M. J. & Kaufman, M. H. Establishment in culture of pluripotential cells from mouse embryos. *Nature* **292,** 154–156 (1981).
2. Tiedemann, H., Asashima, M., Grunz, H. & Knöchel, W. Pluripotent cells (stem cells) and their determination and differentiation in early vertebrate embryogenesis. *Dev. Growth Differ.* **43,** 469–502 (2001).
3. Nichols, J. *et al.* Formation of pluripotent stem cells in the mammalian embryo depends on the POU transcription factor Oct4. *Cell* **95,** 379–391 (1998).
4. Mitsui, K. *et al.* The Homeoprotein Nanog Is Required for Maintenance of Pluripotency in Mouse Epiblast and ES Cells. *Cell* **113,** 631–642 (2003).
5. Masui, S. *et al.* Pluripotency governed by Sox2 via regulation of Oct3/4 expression in mouse embryonic stem cells. *Nat. Cell Biol.* **9,** 625–635 (2007).
6. Takahashi, K. & Yamanaka, S. Induction of pluripotent stem cells from mouse embryonic and adult fibroblast cultures by defined factors. *Cell* **126,** 663–676 (2006).
7. Hanna, J. *et al.* Direct cell reprogramming is a stochastic process amenable to acceleration. *Nature* **462,** 595–601 (2009).
8. Ruiz, S. *et al.* A high proliferation rate is required for cell reprogramming and maintenance of human embryonic stem cell identity. *Curr Biol* **21,** 45–52 (2011).
9. White, J. & Dalton, S. Cell cycle control of embryonic stem cells. *Stem Cell Rev* **1,** 131–138 (2005).
10. Breeden, L. L. Periodic transcription: a cycle within a cycle. *Curr. Biol.* **13,** R31-38 (2003).
11. Ohi, R. & Gould, K. L. Regulating the onset of mitosis. *Curr. Opin. Cell Biol.* **11,** 267–273 (1999).
12. Coverley, D., Laman, H. & Laskey, R. A. Distinct roles for cyclins E and A during DNA replication complex assembly and activation. *Nat. Cell Biol.* **4,** 523–528 (2002).
13. Resnitzky, D., Gossen, M., Bujard, H. & Reed, S. I. Acceleration of the G1/S phase transition by expression of cyclins D1 and E with an inducible system. *Mol. Cell. Biol.* **14,** 1669–1679 (1994).
14. Jeffrey, P. D. *et al.* Mechanism of CDK activation revealed by the structure of a cyclinA-CDK2 complex. *Nature* **376,** 313–320 (1995).
15. Ballabeni, A. *et al.* Cell cycle adaptations of embryonic stem cells. *PNAS* **108,** 19252–19257 (2011).
16. Stead, E. *et al.* Pluripotent cell division cycles are driven by ectopic Cdk2, cyclin A/E and E2F activities. *Oncogene* **21,** 8320–8333 (2002).
17. Savatier, P., Huang, S., Szekely, L., Wiman, K. G. & Samarut, J. Contrasting patterns of retinoblastoma protein expression in mouse embryonic stem cells and embryonic fibroblasts. *Oncogene* **9,** 809–818 (1994).
18. Dalton, S. Linking the Cell Cycle to Cell Fate Decisions. *Trends in Cell Biology* **25,** 592–600 (2015).
19. Fantl, V., Stamp, G., Andrews, A., Rosewell, I. & Dickson, C. Mice lacking cyclin D1 are small and show defects in eye and mammary gland development. *Genes Dev.* **9,** 2364–2372 (1995).

20. Sicinski, P. *et al.* Cyclin D1 provides a link between development and oncogenesis in the retina and breast. *Cell* **82,** 621–630 (1995).
21. Ortega, S. *et al.* Cyclin-dependent kinase 2 is essential for meiosis but not for mitotic cell division in mice. *Nat. Genet.* **35,** 25–31 (2003).
22. Parisi, T. *et al.* Cyclins E1 and E2 are required for endoreplication in placental trophoblast giant cells. *EMBO J.* **22,** 4794–4803 (2003).
23. Geng, Y. *et al.* Cyclin E ablation in the mouse. *Cell* **114,** 431–443 (2003).
24. Murphy, M. *et al.* Delayed early embryonic lethality following disruption of the murine cyclin A2 gene. *Nat. Genet.* **15,** 83–86 (1997).
25. Brandeis, M. *et al.* Cyclin B2-null mice develop normally and are fertile whereas cyclin B1-null mice die in utero. *Proc. Natl. Acad. Sci. U.S.A.* **95,** 4344–4349 (1998).
26. Quelle, D. E. *et al.* Overexpression of mouse D-type cyclins accelerates G1 phase in rodent fibroblasts. *Genes Dev.* **7,** 1559–1571 (1993).
27. Dyson, N. The regulation of E2F by pRB-family proteins. *Genes Dev.* **12,** 2245–2262 (1998).
28. Faast, R. *et al.* Cdk6-cyclin D3 activity in murine ES cells is resistant to inhibition by p16(INK4a). *Oncogene* **23,** 491–502 (2004).
29. Li, V. C., Ballabeni, A. & Kirschner, M. W. Gap 1 phase length and mouse embryonic stem cell self-renewal. *PNAS* **109,** 12550–12555 (2012).
30. Neganova, I. & Lako, M. G1 to S phase cell cycle transition in somatic and embryonic stem cells. *Journal of Anatomy* **213,** 30–44 (2008).
31. Coronado, D. *et al.* A short G1 phase is an intrinsic determinant of naïve embryonic stem cell pluripotency. *Stem Cell Research* **10,** 118–131 (2013).
32. Naumova, N. *et al.* Organization of the Mitotic Chromosome. *Science* **342,** 948–953 (2013).
33. Bernardi, G. Genome Organization and Chromosome Architecture. *Cold Spring Harb Symp Quant Biol* **80,** 83–91 (2015).
34. Oomen, M. E. & Dekker, J. Epigenetic characteristics of the mitotic chromosome in 1D and 3D. *Critical Reviews in Biochemistry and Molecular Biology* **52,** 185–204 (2017).
35. Dixon, J. R. *et al.* Topological domains in mammalian genomes identified by analysis of chromatin interactions. *Nature* **485,** 376–380 (2012).
36. Hsiung, C. C.-S. *et al.* Genome accessibility is widely preserved and locally modulated during mitosis. *Genome Res.* **25,** 213–225 (2015).
37. Liu, Y. *et al.* Transcriptional landscape of the human cell cycle. *PNAS* **114,** 3473–3478 (2017).
38. Xu, J. *et al.* Landscape of monoallelic DNA accessibility in mouse embryonic stem cells and neural progenitor cells. *Nat Genet* **49,** 377–386 (2017).
39. Sarge, K. D. & Park-Sarge, O. K. Gene bookmarking: keeping the pages open. *Trends in Biochemical Sciences* **30,** 605–610 (2005).
40. Sarge, K. D. & Park-Sarge, O.-K. Mitotic bookmarking of formerly active genes: Keeping epigenetic memories from fading. *Cell Cycle* **8,** 818–823 (2009).

41. Zaidi, S. K. *et al.* Mitotic bookmarking of genes: a novel dimension to epigenetic control. *Nat Rev Genet* **11,** 583–589 (2010).
42. Kadauke, S. & Blobel, G. A. Mitotic bookmarking by transcription factors. *Epigenetics & Chromatin* **6,** 6 (2013).
43. Juan, G., Pan, W. & Darzynkiewicz, Z. DNA segments sensitive to single-strand-specific nucleases are present in chromatin of mitotic cells. *Exp. Cell Res.* **227,** 197–202 (1996).
44. Michelotti, E. F., Sanford, S. & Levens, D. Marking of active genes on mitotic chromosomes. *Nature* **388,** 895–899 (1997).
45. Blobel, G. A. *et al.* A Reconfigured Pattern of MLL Occupancy within Mitotic Chromatin Promotes Rapid Transcriptional Reactivation Following Mitotic Exit. *Molecular Cell* **36,** 970–983 (2009).
46. Kadauke, S. *et al.* Tissue-Specific Mitotic Bookmarking by Hematopoietic Transcription Factor GATA1. *Cell* **150,** 725–737 (2012).
47. Caravaca, J. M. *et al.* Bookmarking by specific and nonspecific binding of FoxA1 pioneer factor to mitotic chromosomes. *Genes Dev.* **27,** 251–260 (2013).
48. Lodhi, N., Kossenkov, A. V. & Tulin, A. V. Bookmarking promoters in mitotic chromatin: poly(ADP-ribose)polymerase-1 as an epigenetic mark. *Nucl Acids Res* **42,** 7028–7038 (2014).
49. Festuccia, N. *et al.* Mitotic binding of Esrrb marks key regulatory regions of the pluripotency network. *Nat Cell Biol* **18,** 1139–1148 (2016).
50. Deluz, C. *et al.* A role for mitotic bookmarking of SOX2 in pluripotency and differentiation. *Genes Dev.* **30,** 2538–2550 (2016).
51. Liu, Y. *et al.* Widespread Mitotic Bookmarking by Histone Marks and Transcription Factors in Pluripotent Stem Cells. *Cell Reports* **19,** 1283–1293 (2017).
52. Rothbart, S. B. *et al.* Association of UHRF1 with H3K9 methylation directs the maintenance of DNA methylation. *Nat Struct Mol Biol* **19,** 1155–1160 (2012).
53. Bhatia, S. Transcription Regulation of Pluripotency and Cell Fate. PhD thesis, (2017).
54. M Westendorf, J., N Rao, P. & Gerace, L. Cloning of cDNAs for M-phase phosphoproteins recognized by the MPM2 monoclonal antibody and determination of the phosphorylated epitope. *Proceedings of the National Academy of Sciences of the United States of America* **91,** 714–8 (1994).
55. Buenrostro, J. D., Giresi, P. G., Zaba, L. C., Chang, H. Y. & Greenleaf, W. J. Transposition of native chromatin for fast and sensitive epigenomic profiling of open chromatin, DNA-binding proteins and nucleosome position. *Nat. Methods* **10,** 1213–1218 (2013).
56. Amé, J., Spenlehauer, C. & de Murcia, G. The PARP superfamily. *BioEssays* **26,** 882–893 (2004).
57. Wang, Z. Q. *et al.* PARP is important for genomic stability but dispensable in apoptosis. *Genes Dev.* **11,** 2347–2358 (1997).
58. Wang, Z. Q. *et al.* Mice lacking ADPRT and poly(ADP-ribosyl)ation develop normally but are susceptible to skin disease. *Genes Dev.* **9,** 509–520 (1995).

59. Murcia, J. M. de *et al.* Requirement of poly(ADP-ribose) polymerase in recovery from DNA damage in mice and in cells. *PNAS* **94,** 7303–7307 (1997).
60. Yang, Y.-G., Cortes, U., Patnaik, S., Jasin, M. & Wang, Z.-Q. Ablation of PARP-1 does not interfere with the repair of DNA double-strand breaks, but compromises the reactivation of stalled replication forks. *Oncogene* **23,** 3872–3882 (2004).
61. Bauer, P., Buki, K. & Kun, E. Selective augmentation of histone H1 phosphorylation sites by interaction of poly (ADP-ribose) polymerase and cdc2-kinase: comparison with protein kinase C. *cell cycle* **5,** 6 (2001).
62. Krishnakumar, R. *et al.* Reciprocal Binding of PARP-1 and Histone H1 at Promoters Specifies Transcriptional Outcomes. *Science* **319,** 819–821 (2008).
63. Chiou, S.-H. *et al.* Poly(ADP-ribose) polymerase 1 regulates nuclear reprogramming and promotes iPSC generation without c-Myc. *Journal of Experimental Medicine* **210,** 85–98 (2013).
64. Roper, S. J. *et al.* ADP-ribosyltransferases Parp1 and Parp7 safeguard pluripotency of ES cells. *Nucleic Acids Res* **42,** 8914–8927 (2014).
65. Hemberger, M. *et al.* Parp1-deficiency induces differentiation of ES cells into trophoblast derivatives. *Developmental Biology* **257,** 371–381 (2003).
66. Gibson, B. A. & Kraus, W. L. New insights into the molecular and cellular functions of poly(ADP-ribose) and PARPs. *Nat Rev Mol Cell Biol* **13,** 411–424 (2012).
67. Ji, Y. & Tulin, A. V. The roles of PARP1 in gene control and cell differentiation. *Curr Opin Genet Dev* **20,** 512–518 (2010).
68. Gao, F., Kwon, S. W., Zhao, Y. & Jin, Y. PARP1 Poly(ADP-ribosyl)ates Sox2 to Control Sox2 Protein Levels and FGF4 Expression during Embryonic Stem Cell Differentiation. *J. Biol. Chem.* **284,** 22263–22273 (2009).
69. Lai, Y.-S. *et al.* SRY (sex determining region Y)-box2 (Sox2)/poly ADP-ribose polymerase 1 (Parp1) complexes regulate pluripotency. *PNAS* **109,** 3772–3777 (2012).
70. Liu, Z. & Kraus, W. L. Catalytic-Independent Functions of PARP-1 Determine Sox2 Pioneer Activity at Intractable Genomic Loci. *Molecular Cell* **65,** 589-603.e9 (2017).
71. Wang, Z. Q. *et al.* Mice lacking ADPRT and poly(ADP-ribosyl)ation develop normally but are susceptible to skin disease. *Genes Dev.* **9,** 509–520 (1995).
72. Shieh, W. M. *et al.* Poly(ADP-ribose) Polymerase Null Mouse Cells Synthesize ADP-ribose Polymers. *J. Biol. Chem.* **273,** 30069–30072 (1998).
73. Ménissier de Murcia, J. *et al.* Functional interaction between PARP-1 and PARP-2 in chromosome stability and embryonic development in mouse. *EMBO J.* **22,** 2255–2263 (2003).
74. Ogino, H. *et al.* Loss of Parp-1 affects gene expression profile in a genome-wide manner in ES cells and liver cells. *BMC Genomics* **8,** 41 (2007).
75. Teves, S. S. *et al.* A dynamic mode of mitotic bookmarking by transcription factors. *eLife* **5,** e22280 (2016).

76. O'Connor, M. D. *et al.* Alkaline Phosphatase-Positive Colony Formation Is a Sensitive, Specific, and Quantitative Indicator of Undifferentiated Human Embryonic Stem Cells. *STEM CELLS* **26,** 1109–1116 (2008).
77. Abouzied, M. M. *et al.* Hepatoma-derived Growth Factor SIGNIFICANCE OF AMINO ACID RESIDUES 81–100 IN CELL SURFACE INTERACTION AND PROLIFERATIVE ACTIVITY. *J. Biol. Chem.* **280,** 10945–10954 (2005).
78. Gijsbers, R. *et al.* Role of the PWWP Domain of Lens Epithelium-derived Growth Factor (LEDGF)/p75 Cofactor in Lentiviral Integration Targeting. *J. Biol. Chem.* **286,** 41812–41825 (2011).
79. Wu, H. *et al.* Structural and Histone Binding Ability Characterizations of Human PWWP Domains. *PLOS ONE* **6,** e18919 (2011).
80. Maurer-Stroh, S. *et al.* The Tudor domain 'Royal Family': Tudor, plant Agenet, Chromo, PWWP and MBT domains. *Trends Biochem. Sci.* **28,** 69–74 (2003).
81. Kishima, Y. *et al.* Hepatoma-derived Growth Factor Stimulates Cell Growth after Translocation to the Nucleus by Nuclear Localization Signals. *J. Biol. Chem.* **277,** 10315–10322 (2002).
82. Abouzied, M. M. *et al.* Expression patterns and different subcellular localization of the growth factors HDGF (hepatoma-derived growth factor) and HRP-3 (HDGF-related protein-3) suggest functions in addition to their mitogenic activity. *Biochemical Journal* **378,** 169–176 (2004).
83. Everett, A. D., Yang, J., Rahman, M., Dulloor, P. & Brautigan, D. L. Mitotic phosphorylation activates hepatoma-derived growth factor as a mitogen. *BMC Cell Biology* **12,** 15 (2011).
84. Gallitzendoerfer, R. *et al.* Hepatoma-derived growth factor (HDGF) is dispensable for normal mouse development. *Dev. Dyn.* **237,** 1875–1885 (2008).
85. Sedlmaier, A. *et al.* Overexpression of hepatoma-derived growth factor in melanocytes does not lead to oncogenic transformation. *BMC Cancer* **11,** 457 (2011).
86. Zhao, J. *et al.* Interactome study suggests multiple cellular functions of hepatoma-derived growth factor (HDGF). *Journal of Proteomics* **75,** 588–602 (2011).
87. Enomoto, H., Nakamura, H., Liu, W. & Nishiguchi, S. Hepatoma-Derived Growth Factor: Its Possible Involvement in the Progression of Hepatocellular Carcinoma. *International Journal of Molecular Sciences* **16,** 14086–14097 (2015).
88. Gijsbers, R. *et al.* LEDGF Hybrids Efficiently Retarget Lentiviral Integration Into Heterochromatin. *Molecular Therapy* **18,** 552–560 (2010).
89. Gijsbers, R. *et al.* Role of the PWWP Domain of Lens Epithelium-derived Growth Factor (LEDGF)/p75 Cofactor in Lentiviral Integration Targeting. *J. Biol. Chem.* **286,** 41812–41825 (2011).
90. Pradeepa, M. M., Sutherland, H. G., Ule, J., Grimes, G. R. & Bickmore, W. A. Psip1/Ledgf p52 Binds Methylated Histone H3K36 and Splicing Factors and Contributes to the Regulation of Alternative Splicing. *PLOS Genetics* **8,** e1002717 (2012).

91. Van Nuland, R. *et al.* Nucleosomal DNA binding drives the recognition of H3K36-methylated nucleosomes by the PSIP1-PWWP domain. *Epigenetics & Chromatin* **6,** 12 (2013).
92. Sutherland, H. G. *et al.* Disruption of Ledgf/Psip1 Results in Perinatal Mortality and Homeotic Skeletal Transformations. *Mol. Cell. Biol.* **26,** 7201–7210 (2006).
93. Pradeepa, M. M. *et al.* Psip1/p52 regulates posterior Hoxa genes through activation of lncRNA Hottip. *PLOS Genetics* **13,** e1006677 (2017).
94. Yang, J. & Everett, A. D. Hepatoma-derived growth factor binds DNA through the N-terminal PWWP domain. *BMC Mol. Biol.* **8,** 101 (2007).